JOURNAL OF NATURAL PRODUCTS

Article

pubs.acs.org/jnp

Myrsinane, Premyrsinane, and Cyclomyrsinane Diterpenes from *Euphorbia falcata* as Potassium Ion Channel Inhibitors with Selective G Protein-Activated Inwardly Rectifying Ion Channel (GIRK) Blocking Effects

Andrea Vasas,[†] Peter Forgo,[†] Péter Orvos,[‡,§] László Tálosi,[‡] Attila Csorba,[†] Gyula Pinke,[⊥] and Judit Hohmann*[,†,∥]

[†]Department of Pharmacognosy and [∥]Interdisciplinary Centre for Natural Products, University of Szeged, Eötvös u. 6, H-6720 Szeged, Hungary

[‡]Rytmion Ltd., Ősz u. 27, H-6724 Szeged, Hungary

[§]Department of Pharmacology and Pharmacotherapy, University of Szeged, Dóm tér 12, H-6720 Szeged, Hungary

[⊥]Department of Botany, Faculty of Agricultural and Food Sciences, Széchenyi István University, Vár 2, H-9200 Mosonmagyaróvár, Hungary

Supporting Information

ABSTRACT: GIRK channels are activated by a large number of G protein-coupled receptors and regulate the electrical activity of neurons, cardiac atrial myocytes, and β-pancreatic cells. Abnormalities in GIRK channel function have been implicated in the pathophysiology of neuropathic pain, drug addiction, and cardiac arrhythmias. In the heart, GIRK channels are selectively expressed in the atrium, and their activation inhibits pacemaker activity, thereby slowing the heart rate. In the present study, 19 new diterpenes, falcatins A–S (**1**–**19**), and the known euphorprolitherin D (**20**) were isolated from *Euphorbia falcata*. The compounds were assayed on stable transfected HEK-hERG (Kv11.1) and HEK-GIRK1/4 (Kir3.1 and Kir3.4) cells. Blocking activity on GIRK channels was exerted by 13 compounds (61–83% at 10 μM), and, among them, five possessed low potency on the hERG channel (4–20% at 10 μM). These selective activities suggest that myrsinane-related diterpenes are potential lead compounds for the treatment of atrial fibrillation.

falcatin A (**1**)

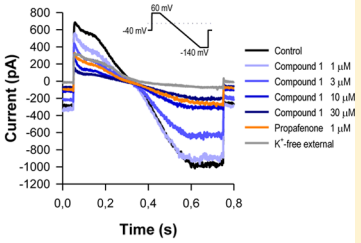

Cardiovascular diseases are the leading cause of death and loss of disability-adjusted life-years worldwide.[1] A notable portion of such diseases are linked to the dysfunction of cardiac ion channels. Ion channels are a large and diverse family of transmembrane pore-forming proteins.[2−8] These proteins facilitate the rapid passive transport of specific inorganic ions (such as Na^+, K^+, Ca^{2+}, and Cl^-) through the lipid bilayers of plasma and organelle membranes down their electrochemical gradient that is established by the work of pumps and transporters.[2,6−10] Defined by the stimulus necessary to evoke activity, the majority of ion channels are classified commonly into two main subgroups: voltage-gated and ligand-gated channels. The most important difference is that voltage-gated ion channels are activated by changes in plasma membrane potential, while ligand-gated channels are activated by endogenous ligands.[4−11] Ion channels are also grouped into various subclasses by another key functional characteristic, their selective permeability to different ions.[8,9,12] Voltage-gated ion channels are rather specific for the various cations and anions. Therefore, these channels are typically named after the ion for which they are selective. Several classes of potassium channels play an important role in the regulation of function of the myocardium.

GIRK channels (G protein-activated inwardly rectifying potassium ion channels) are involved in the regulation of the electrical activity of neurons, cardiac atrial myocytes, and β-pancreatic cells. Abnormalities in GIRK channel function have been implicated in the pathophysiology of neuropathic pain, drug addiction, cardiac arrhythmias, and other disorders.[13] In the heart muscles, GIRK potassium channels are selectively expressed in the cardiac atrium, activated by a large number of G protein-coupled receptors and responsible for K^+-fluxes and membrane repolarization and/or hyperpolarization. Electrical remodeling of atrial heart muscle during chronic atrial fibrillation may result in a constitutively active form of the GIRK channel, which may lead to an important role of this channel in this disease. Selective

Received: March 22, 2016

DOI: 10.1021/acs.jnatprod.6b00260
J. Nat. Prod. XXXX, XXX, XXX−XXX

inhibition of myocardial GIRK channels in animal atrial fibrillation models reduces the number of provoked atrial fibrillation episodes and decreases the duration of these arrhythmic periods. Therefore, selective blockade of the GIRK channel might be a useful tool in the treatment of atrial fibrillation, and these channels are novel targets in the search for new antiarrhythmic agents.[14−16]

hERG channels (human ether-a-go-go-related gene encoded potassium channels) are K^+-selective voltage-gated ion channels, belonging to the Kv channel family, also referred to as Kv11.1. hERG channels mediate the rapid delayed rectifier K^+ current (I_{Kr}) in ventricular myocytes and are expressed in both the atrium and ventricle. These channels can be blocked by chemicals with diverse structures that encompass several therapeutic drug classes, including antiarrhythmics, psychiatric agents, antimicrobials, and antihistamines.[17] Compounds with hERG-blocking activity may modify the action potential of the heart muscle, which can lead to prolongation of the action potential and an increased risk of severe ventricular arrhythmias such as ventricular fibrillation and sudden cardiac death. hERG-blocking activity has been the reason for the withdrawal of several would-be "blockbuster" drugs from the market. At present, every new drug must go through preclinical safety testing determined by the U.S. Food and Drug Administration, the European Medicines Agency, and other regulatory entities.[2,3,5,8,18−20]

For many years natural products have made a major impact in the treatment of cardiovascular diseases. More recently, a number of bioactive compounds generally obtained from terrestrial plants such as carotenoids, catechin, isoflavones, quercetin, resveratrol, sulforaphane, and tocotrienols have been proven to promote cardioprotection and to reduce the risk of cardiovascular diseases.[21] Great efforts are ongoing worldwide in the search for new natural compounds that can selectively influence these diseases.

Plants in the genus *Euphorbia* are well known for the chemical diversity of their diterpenoids. Several of them are of particular interest because of their restricted occurrence and broad structural diversity, as a consequence of different frameworks such as jatrophanes, tiglianes, ingenanes, lathyranes, myrsinanes, and daphnanes.[22] Previous studies have indicated that diterpenes of *Euphorbia* species have a wide variety of biological activities, such as skin-irritant, antiproliferative, cytotoxic, and antiviral properties and multidrug resistance modulating and anti-inflammatory effects.[22−24] However, no data have been reported concerning the potential cardiac effects of this type of natural compound.

As a part of our research program to discover new bioactive compounds from *Euphorbia* species, the chloroform-soluble fraction of a methanol extract of *Euphorbia falcata* L. (Euphorbiaceae) was investigated. This study resulted in the isolation and structure determination from this plant of 19 new diterpenes (falcatins A−S, **1**−**19**) and one known diterpene (euphorprolitherin D, **20**) based on myrsinane, premyrsinane, and cyclomyrsinane skeletons. These compounds together with four premyrsinane and cyclomyrsinane-type diterpenes (**21**−**24**),[25,26] isolated earlier from this plant by our group, were studied for their GIRK- and hERG channel-inhibitory activities using an automated patch-clamp method.

RESULTS AND DISCUSSION

Twenty diterpenes (**1**−**20**) were isolated from the $CHCl_3$-soluble phase of the MeOH extract prepared from the whole plant of *E. falcata* by a combination of different chromatographic methods, such as CC, VLC, CPC, preparative TLC, and HPLC. The structure elucidation was carried out by spectroscopic analysis, including 1D and 2D NMR (^{1}H−^{1}H COSY, HSQC, HMBC, and NOESY) and HRESIMS experiments. The NMR data showed that all compounds are myrsinane-related diterpenes (myrsinanes, premyrsinanes, and cyclomyrsinanes).

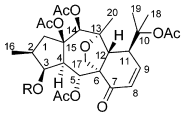

	R
1	Bz
2	Prop
3	*i*Bu

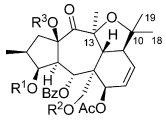

	R^1	R^2	R^3
4	Prop	*i*Bu	Ac
5	*i*Bu	Ac	Ac
6	*i*Bu	*i*Bu	H

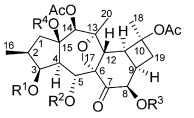

	R^1	R^2	R^3	R^4
7	Ac	Bz	Bz	Ac
8	*i*Bu	Ac	Ac	Ac
9	Nic	Ac	MeBu	Ac
20	Prop	Ac	Bz	H

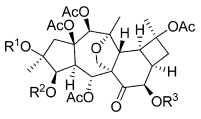

	R^1	R^2	R^3
10	H	Prop	MeBu
11	H	*i*Bu	MeBu
12	Nic	*i*Bu	MeBu
13	Nic	*i*Bu	*i*Bu
14	Nic	Prop	*i*Bu
15	Bz	Prop	MeBu

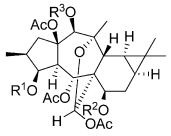

	R^1	R^2	R^3
16	*i*Bu	Bz	Ac
17	*i*Bu	Nic	Bz
18	Prop	Nic	Bz

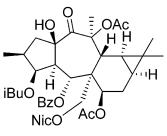

19

Characterization of Compounds 1−19. Compound **1** was obtained as an amorphous solid with $[\alpha]^{25}_D$ −8 (*c* 0.2, $CHCl_3$). Its HRESIMS provided the molecular formula, $C_{35}H_{42}O_{12}$, through the presence of a peak at *m/z* 677.2594 $[M + Na]^+$ (calcd for $C_{35}H_{42}O_{12}Na$, 677.2574). The ^{1}H and ^{13}C NMR spectra of **1** revealed the presence of four acetyl groups [δ_H 1.97 s, 2.01 s, 2.06, and 2.16 s; δ_C 170.5, 169.2, 170.1, and 168.3 (CO) and 22.4, 21.1, 21.0, and 23.2 (CH_3)] and one benzoyl substituent [δ_H 7.94 d, 7.40 and 7.53 t; δ_C 166.8, 129.3, 128.0, 132.6, and 131.0] (Tables 1 and 2). Additionally, the ^{1}H NMR spectrum exhibited signals attributed to skeletal protons, including four methyls (0.88 d, 1.59 s, 1.45 s, and 1.24 s). The ^{1}H−^{1}H COSY spectrum defined two structural fragments with correlated protons: −CH_2−CH(CH_3)−CHR−CH−CHR− (A) (δ_H 2.83, 2.61, 2.27, 5.63, 3.15, and 6.00) and −CH=CH− (B) (δ_H 6.19 and 6.54). These two structural parts and the tertiary methyls and quaternary carbons were connected by inspection of the long-range C−H correlations observed in the HMBC spectrum (Figure 1). The two- and three-bond correlations between the quaternary carbon C-15 and H-1, H-3, and H-4 and between C-4 and H-1 and H-5 revealed that structural fragment A together with C-15 forms a five-membered ring, present in many types of Euphorbiaceae diterpenes. HMBC cross-peaks

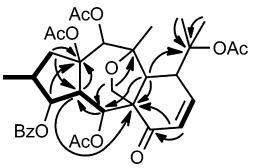

Figure 1. Selected ^{1}H−^{1}H COSY (bold) and HMBC (C→H) correlations for **1**.

DOI: 10.1021/acs.jnatprod.6b00260
J. Nat. Prod. XXXX, XXX, XXX−XXX

Table 1. ^{1}H NMR Data (δ_H) of Compounds 1−6 [δ ppm (J = Hz), $CDCl_3$, 500 MHz]

position	1	2	3	4	5	6
1α	2.83, dd (15.8, 10.9)	2.80, dd (15.8, 9.8)	2.76, dd (15.8, 10.9)	3.06, dd (14.5, 9.0)	3.14, dd (14.4, 5.6)	2.92, m
1β	2.61, dd (15.8, 9.1)	2.50, dd (15.8, 9.3)	2.54, m	1.75, dd (14.5, 9.2)	1.76, dd (14.4, 10.1)	1.75, dd (14.5, 9.3)
2	2.27, m	2.18, m	2.16, m	2.13, m	2.15, m	2.09, m
3	5.63, t (3.8)	5.41, t (3.4)	5.39, t (3.5, 3.2)	5.51, t (4.4)	5.53, t (4.1)	5.55, t (3.8)
4	3.15, dd (10.9, 3.7)	3.00, dd (10.8, 3.4)	3.01, dd (10.9, 3.6)	2.91, m	2.84, dd (11.0, 4.2)	3.04, dd (11.1, 3.8)
5	6.00, d (10.9)	5.92, d (10.8)	5.90, d (10.9)	6.50, d (11.3)	6.49, d (11.1)	6.48, d (11.1)
7				5.16, d (5.3)	5.21, d (5.3)	5.07, d (5.3)
8	6.19, d (10.3)	6.22, d (10.3)	6.20, d (10.2)	6.01, m	6.04, m	6.02, m
9	6.54, dd (10.3, 6.2)	6.57, dd (10.3, 6.4)	6.55, dd (10.2, 6.3)	5.87, dd (9.8, 1.9)	5.87, d (9.8)	5.84, d (9.8)
11	3,07, brm	3.06, brm	3.03, brm	2.91, m	2.88, d (12.8)	2.92, m
12	3.58, s	3.54, s	3.53, s	3.45, d (12.7)	3.42, d (12.8)	3.20, d (12.7)
14	5.13, s	5.08, s	5.06, s			
16	0.88, d (6.8)	0.84, d (6.8)	0.82, d (6.8)	0.92, d (6.9)	0.88, d (7.0)	0.90, d (6.8)
17	4.31, d (9.1)	4.28, d (9.0)	4.26, d (9.1)	4.48, d (12.1)	4.59, d (12.1)	4.50, d (12.0)
	3.87, d (9.1)	3.87, d (9.0)	3.84, d (9.1)	4.29, d (12.1)	4.12, d (12.1)	4.32, d (12.0)
18	1.59, s	1.59, s	1.57, s	1.04, s	1.03, s	1.06, s
19	1.45, s	1.46, s	1.45, s	1.44, s	1.43, s	1.45, s
20	1.24, s	1.23, s	1.22, s	1.57, s	1.60, s	1.54, s
*Oi*Bu-3						
2			2.58, sept (7.0)		2.43, m	2.47, sept (7.0)
3			1.18, d (7.0)		1.13, d (7.1)	1.14, d (7.1)
4			1.18, d (7.0)		0.93, d (7.0)	0.99, d (6.9)
*O*Prop-3						
2		2.43, dq, 2.31, dq (16.6, 7.8)		2.22, m (2H)		
3		1.16, t (7.8)		0.94, t (7.2)		
*O*Ac-5	2.01, s	2.03, s	2.01, s		2.24, s	
*O*Ac-7				2.24, s		2.17, s
*O*Ac-10	1.97, s	2.02, s	2.00, s			
*O*Ac-14	2.06, s	2.06, s	2.04, s			
*O*Ac-15	2.16, s	2.10, s	2.09, s	2.22, s	2.22, s	
*O*Ac-17					1.54, s	
*O*iBu-17						
2				2.09, sept (6.8)		2.20, m
3				0.96, d (6.8)		0.99, d (6.9)
4				0.93, d (6.9)		0.95, d (6.9)
*O*Bz						
2, 6	7.94, d (7.0)			7.88, d (7.1)	7.89, d (7.3)	7.88, d (7.4)
3, 5	7.40, t (7.8)			7.39, t (7.8)	7.54, t (7.4)	7.39, t (7.6)
4	7.53, t (7.5)			7.53, t (7.5)	7.40, t (7.7)	7.53, t (7.3)
OH-15						2.83, s

between C-6 and H-4, H-8, and H-12, between C-7 and H-8, and between C-10 and H-12, H-18, and H-19 established a 10,18-dihydromyrsinol-type diterpene with O-functionalities at C-3, C-5, C-7, C-10, C-14, and C-15. Moreover, the heteronuclear long-range coupling between C-5 and H-17 and H-12, C-6 and H-17 and H-12, and between C-13 and H-17 indicated an O-bridge between C-17 and C-13, which is characteristic of many myrsinane, cyclomyrsinane, and premyrsinane polyesters. The positions of the ester groups were established via the HMBC experiment. The correlations of the carbonyl signal at δ_C 169.2 with the proton signal at δ_H 6.00 (H-5) and the acetyl methyl signal at δ_H 2.01, and the carbonyl signal at δ_C 170.1 with the proton signal at δ_H 5.13 (H-14) and the acetyl methyl signal at δ_H 2.06, indicated the presence of two acetyl groups at C-5 and C-14. Similarly, the HMBC cross-peak of the signal at δ_C 166.8 (benzoyl CO) with the proton signals at δ_H 5.63 (H-3) demonstrated the presence of the benzoyl group at C-3. The acetyl group at C-15 was indicated by the weak four-bond HMBC correlation between C-15 and the acetyl methyl signal at δ_H 2.16. Furthermore, the position of the OAc-15 group was corroborated by the NOESY correlations between Bz-2′,6′ and OAc-15.

The relative configuration of **1** was elucidated as follows. For the reported natural myrsinol diterpenes, the three rings (5/7/6) forming the myrsinol skeleton are *trans*-fused, H-4 and H_2-17 are α-oriented, and Me-16, H-12, the side chain at C-11, and the C-15 acetyl group are β-oriented (Figure 2).[27] NOESY correlations of **1** observed for H-2/H-3, H-3/H-4, H-4/H-14, H-4/H-2, and H-14/H-1b suggested that H-1b, H-2, H-3, H-4, and H-14 are α-oriented, while correlations between H-1a/H_3-16 and H-5/H-12 proved the β-orientation of H-1a and H-5.

This stereochemistry of **1** was in agreement with the configuration of 10,18-dihydromyrsinol diterpenes reported earlier.[28,29] All of the above evidence confirmed the structure of **1** as 5α,10,14β,15β-*O*-tetraacetyl-3β-*O*-benzoyl-10,18-dihydromyrsinol, which was named falcatin A.

Compound **2** was obtained as an amorphous solid with $[\alpha]^{28}_D$ +22 (c 0.1, $CHCl_3$). It was found to possess a molecular formula

DOI: 10.1021/acs.jnatprod.6b00260
J. Nat. Prod. XXXX, XXX, XXX−XXX

Table 2. ^{13}C NMR Data (δ_C) of Compounds 1−6 ($CDCl_3$, 125 MHz)

position	1	2	3	4	5	6
1	44.3, CH_2	43.8, CH_2	44.0, CH_2	42.8, CH_2	n.d.[a]	46.3, CH_2
2	36.5, CH	35.9, CH	36.1, CH	36.0, CH	n.d.[a]	36.0, CH
3	76.7, CH	76.0, CH	75.8, CH	77.2, CH	77.0, CH	78.4, CH
4	52.4, CH	52.4, CH	52.2, CH	50.9, CH	51.4, CH	50.1, CH
5	66.8, CH	67.0, CH	66.8, CH	68.8, CH	69.1, CH	69.0, CH
6	61.8, C	61.7, C	61.7, C	47.0, C	n.d.[a]	47.1, C
7	197.3, C	197.3, C	197.3, C	68.2, CH	68.0, CH	68.3, CH
8	131.6, CH	131.7, CH	131.6, CH	126.1, CH	126.3, CH	126.3, CH
9	140.7, CH	140.8, CH	140.7, CH	129.0, CH	128.9, CH	128.9, CH
10	85.4, C	85.5, C	85.3, C	79.3, C	80.8, C	79.2, C
11	42.5, CH	n.d.[a]	n.d.[a]	47.4, CH	47.7, CH	47.6, CH
12	41.7, CH	41.5, CH	41.5, CH	41.8, CH	42.1, CH	41.7, CH
13	89.3, C	89.2, C	89.3, C	84.6, C	85.5, C	85.3, C
14	81.1, CH	81.0, CH	81.0, CH	200.2, C	201.5, C	205.3, C
15	90.4, C	90.5, C	90.3, C	88.9, C	90.4, C	83.6, C
16	14.2, CH_3	14.2, CH_3	14.0, CH_3	14.3, CH_3	14.5, CH_3	14.5, CH_3
17	72.2, CH_2	72.2, CH_2	72.1, CH_2	61.4, CH_2	61.3, CH_2	61.6, CH_2
18	23.6, CH_3	23.8, CH_3	23.7, CH_3	24.8, CH_3	25.0, CH_3	24.6, CH_3
19	24.0, CH_3	24.0, CH_3	23.9, CH_3	29.7, CH_3	29.4, CH_3	29.5, CH_3
20	23.6, CH_3	23.0, CH_3	23.5, CH_3	26.1, CH_3	26.0, CH_3	24.7, CH_3
*Oi*Bu-3 1			176.6, C			175.2, C
2			34.3, CH			34.1, CH
3			19.3, CH_3			19.3, CH_3
4			19.3, CH_3			19.0, CH_3
*O*Ac-5	169.2, C	169.4, C	169.4, C			
	21.1, CH_3	21.2, CH_3	21.2, CH_3			
*O*Ac-7				170.0, C	171.4, C	170.0, C
				21.2, CH_3	21.5, CH_3	21.2, CH_3
*O*Ac-10	170.5, C	170.4, C	170.4, C			
	22.4, CH_3	22.5, CH_3	22.4, CH_3			
*O*Ac-14	170.1, C	170.1, C	170.1, C			
	21.0, CH_3	21.0, CH_3	21.0, CH_3			
*O*Ac-15	168.3, C	168.3, C	168.3, C	168.0, C	170.1, C	
	23.2, CH_3	23.0, CH_3	22.9, CH_3	21.4, CH_3	20.6, CH_3	
*O*Ac-17					171.9, C	
					21.5, CH_3	
*O*Bz CO	166.8, C			165.5, C	166.6, C	165.0, C
1	131.0, C			129.7, C	130.7, C	129.7, C
2, 6	129.3, CH			129.6, CH	129.8, CH	129.6, CH
3, 5	128.0, CH			128.3, CH	128.5, CH	128.3, CH
4	132.6, CH			133.3, CH	133.3, CH	133.2, CH
*Oi*Bu-3 1					177.2, C	
2					35.6, CH	
3					20.7, CH_3	
4					19.5, CH_3	
*Oi*Bu-17 1				176.5, C		176.5, C
2				33.9, CH		33.8, CH
3				19.0, CH_3		19.0, CH_3
4				18.2, CH_3		17.6, CH_3
*O*Prop-3 1		174.8, C		173.1, C		
2		27.7, CH_2		27.4, CH_2		
3		9.0, CH_3		8.7, CH_3		

[a]n.d., not detected.

of $C_{31}H_{42}O_{12}$ based on the HRESIMS [m/z 629.2600 $[M + Na]^+$ (calcd for $C_{31}H_{42}O_{12}Na$, 629.2574)]. The ^1H NMR and JMOD spectra of **2** revealed four acetate [δ_H 2.02 s, 2.03 s, 2.06 and 2.10 s; δ_C 170.4, 169.4, 170.1, and 168.3 (CO) and 22.5, 21.2, 21.0, and 23.0 (CH_3)] and one propanoate [δ_H 2.43 dq, 2.31 dq and 1.16 t; δ_C 174.8, 27.7, and 9.0] group (Tables 1 and 2). Additionally, the spectra exhibited resonances closely related to those of **1**.

After the ^1H and ^{13}C NMR data on **2** had been assigned by analysis of its $^1H-^1H$ COSY, HSQC, and HMBC spectra, it was obvious that compounds **1** and **2** are based on the same parent system and differ only in the substitution on C-3. The absence of

DOI: 10.1021/acs.jnatprod.6b00260
J. Nat. Prod. XXXX, XXX, XXX−XXX

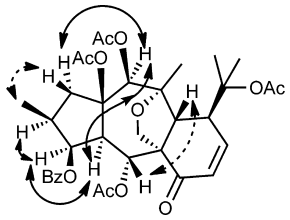

Figure 2. Diagnostic NOESY correlations of **1**.

signals for a benzoate group and the appearance of signals of a propanoate group indicated the replacement of a benzoate residue with a propanoate group. The position of the propanoyl group at C-3 was corroborated by the HMBC cross-peak between δ_H 5.41 (H-3) and the carbon signal at δ_C 174.8 (propanoyl CO). In the case of the acetyl groups, weak $^4J_{C,H}$ couplings were also detected in the HMBC spectrum between C-5, C-10, and C-14 and the corresponding acetate methyl protons, proving unequivocally the locations of acetate groups.

Table 3. ^{1}H NMR Data (δ_H) of Compounds 7−12 ($CDCl_3$, 500 MHz[a] or 600 MHz[b])

position	7[b]	8[a]	9[a]	10[a]	11[a]	12[a]
1α	2.89, dd (15.5, 11.5)	2.55, m	2.93, dd (15.9, 11.0)	3.69, d (16.3)	3.67, d (16.3)	2.84, d (16.7)
1β	2.29, m	2.78, m	2.66, m	1.97, d (16.3)	2.00, d (16.2)	3.83, d (16.8)
2	2.22, m	2.20, m	2.33, m			
3	5.68, t (3.0)	5.44, t (3.9)	5.73, t (3.7)	5.02, d (6.2)	5.02, d (6.2)	5.61, d (4.3)
4	3.16, dd (11.0, 3.0)	2.97, dd (11.0, 3.9)	3.10, dd (10.6, 3.6)	2.94, dd (10.5, 6.2)	2.98, dd (10.8, 6.2)	3.20, dd (10.9, 4.4)
5	6.13, d (11.0)	5.90, d (11.0)	5.86, d (10.6)	5.93, d (10.5)	5.93, d (10.8)	5.91, d (10.7)
8	5.00, d (7.2)	5.25, d (6.9)	5.21, d (7.0)	5.29, d (6.6)	5.29, d (6.7)	5.27, d (6.9)
9	2.81, m	2.75, m	2.73, m	2.75, m	2.70, m	2.75, m
11	2.36, m	2.41, dt (12.5, 2.0)	2.40, m	2.45, m	2.50, dd (10.5, 7.4)	2.48, m
12	3.99, d (12.6)	4.09, d (12.5)	4.10, d (12.3)	3.96, d (12.2)	3.96, d (12.3)	4.01, d (12.3)
14	5.05, s	5.04, s	5.12, s	4.94, s	4.95, s	5.05, s
16	0.87, d (6.6)	0.86, d (6.8)	0.94, d (6.7)	1.46, s	1.46, s	1.79, s
17	4.29, d (9.6)	4.21, d (9.8)	4.26, d (9.8)	4.24, d (9.8)	4.24, d (9.8)	4.27, d (9.9)
	3.61, d (9.6)	3.60, d (9.8)	3.61, d (9.8)	3.59, d (9.8)	3.60, d (9.8)	3.62, d (9.9)
18	1.57, s	1.64, s	1.64, s	1.66, s	1.64, s	1.65, s
19	2.58, m	2.53, m	2.50, m	2.52, d (9.2)	2.52, m	2.52, d (9.1)
20	1.14, s	1.20, s	1.22, s	1.18, s	1.26, s	1.20, s
*Oi*Bu-3						
2		2.46, sept (7.1)			2.51, sept (7.0)	2.42, m
3		1.17, d (7.1)			1.18, d (7.1)	1.06, d (6.9)
4		1.14, d (6.9)			1.10, d (6.9)	1.00, d (7.2)
*O*Prop-3						
2				2.28, q (7.6)		
3				1.10, t (7.6)		
*O*Ac-3	2.01, s					
*O*Ac-5		1.92, s	1.95, s	1.90, s	1.89, s	1.96, s
*O*Ac-8		2.27, s				
*O*Ac-10	1.92, s	2.10, s	2.11, s[c]	2.09, s	2.09, s	2.08, s
*O*Ac-14	2.02, s	2.10, s	2.13, s	2.09, s	2.09, s	2.11, s
*O*Ac-15	1.53, s	2.20, s	2.30, s[c]	2.18, s	2.19, s	2.16, s
*O*Bz-5						
2, 6	7.88, d (6.6)					
3, 5	6.46, t (7.8)					
4	7.12, t (7.8)					
*O*MeBu-8						
2			2.20, m	2.67, m	2.65, m	2.62 m
3			1.55, m; 1.40, m	1.75, m; 1.60, m	1.75, m; 1.58, m	1.63, m; 1.72, m
4			0.78, t (7.4)	0.92, t (7.5)	0.92, t (7.5)	0.87, t (7.4)
5			0.60, d (6.8)	1.31, d (6.9)	1.32, d (6.9)	1.25, d (6.9)
*O*Nic						
2			9.10, s			9.06, s
4			8.29, d (8.0)			8.14, d (8.0)
5			7.40, dd (7.8, 4.8)			7.35, dd (7.8, 4.9)
6			8.78, d (4.8)			8.75, d (4.9)
*O*Bz-8						
2, 6	7.88, d (6.6)					
3, 5	7.43, t (7.2)					
4	7.62, t (7.2)					

[c]Data are interchangeable.

DOI: 10.1021/acs.jnatprod.6b00260
J. Nat. Prod. XXXX, XXX, XXX−XXX

Table 4. ^{13}C NMR Data (δ_C) of Compounds 7−12 ($CDCl_3$, 125 MHz[a] or 150 MHz[b])

position	7[b]	8[a]	9[a]	10[a]	11[a]	12[a]
1	43.2, CH_2	43.1, CH_2	43.3, CH_2	51.0, CH_2	51.0, CH_2	48.3, CH_2
2	37.2, CH	36.3, CH	36.4, CH	75.3, C	75.5, C	85.0, C
3	78.0, CH	76.7, CH	78.4, CH	80.1, CH	80.0, CH	78.2, CH
4	51.4, CH	51.0, CH	51.5, CH	49.6, CH	49.4, CH	47.2, CH
5	68.3, CH	68.9, CH	68.5, CH	69.5, CH	69.5, CH	68.4, CH
6	62.3, C	62.2, C	62.1, C	62.3, C	62.3, C	62.5, C
7	204.3, C	204.4, C	204.4, C	204.7, C	204.7, C	204.2, C
8	74.3, CH	71.4, CH	70.8, CH	71.3, CH	71.3, CH	71.2, CH
9	30.7, CH	29.8, CH	30.0, CH	30.1, CH	30.1, CH	30.1, CH
10	77.8, C	77.5, C	77.5, C	77.5, C	77.6, C	77.6, C
11	42.0, CH	41.8, CH	41.9, CH	41.5, CH	41.6, CH	41.8, CH
12	41.1, CH	41.4, CH	41.3, CH	41.3, CH	41.3, CH	41.5, CH
13	89.6, C	89.3, C	89.4, C	88.6, C	88.7, C	89.3, C
14	81.9, CH	81.9, CH	82.0, CH	80.8, CH	81.0, CH	81.9, CH
15	89.9, C	90.3, C	90.5, C	89.9, C	89.9, C	88.6, C
16	13.9, CH_3	13.9, CH_3	14.1, CH_3	29.7, CH_3	29.7, CH_3	25.0, CH_3
17	67.4, CH_2	67.1, CH_2	67.1, CH_2	66.9, CH_2	67.0, CH_2	67.3, CH_2
18	24.0, CH_3	24.4, CH_3	24.4, CH_3	24.6, CH_3	24.6, CH_3	24.6, CH_3
19	37.1, CH_2	35.0, CH_2	34.9, CH_2	35.0, CH_2	35.0, CH_2	35.3, CH_2
20	21.7, CH_3	22.2, CH_3	22.3, CH_3	22.0, CH_3	22.3, CH_3	22.4, CH_3
*O*Ac-3	169.9, C					
	21.0, CH_3					
*O*Ac-5		170.0, C	169.2, C	169.5, C	169.5, C	169.7, C
		20.7, CH_3	20.8, CH_3	20.7, CH_3	20.6, CH_3	20.9, CH_3
*O*Ac-8		168.5, C				
		21.3, CH_3				
*O*Ac-10	168.9, C	169.0, C	169.2, C	168.7, C	168.7, C	168.8, C
	21.7, CH_3	21.3, CH_3	21.3, CH_3	21.3, CH_3	21.3, CH_3	21.3, CH_3
*O*Ac-14	170.7, C	170.6, C	170.6, C	170.2, C	170.2, C	170.3, C
	21.3, CH_3	21.7, CH_3	21.7, CH_3	21.3, CH_3	21.6, CH_3	21.7, CH_3
*O*Ac-15	167.5, C	167.9, C	168.1, C	169.2, C	169.1, C	168.2, C
	22.6 CH_3	23.5, CH_3	23.4, CH_3	23.2, CH_3	23.2, CH_3	23.2, CH_3
*O*Prop-3 1				174.3, C		
2				27.1, CH_2		
3				8.9, CH_3		
*Oi*Bu-3 1		176.0, C			177.1, C	175.3, C
2		34.3, CH			33.9, CH	34.1, CH
3		18.6, CH_3			19.6, CH_3	18.4, CH_3
4		19.4, CH_3			18.2, CH_3	19.0, CH_3
*O*Bz-5 *CO*	166.0, C					
1	129.5, C					
2, 6	129.6, CH					
3, 5	128.1, CH					
4	132.8, CH					
*O*MeBu-8 1			174.6, C	174.5, C	174.6, C	174.6, C
2			40.9, CH	41.0, CH	41.0, CH	41.1, CH
3			26.9, CH_2	27.0, CH_2	27.0, CH_2	27.0, CH_2
4			11.0, CH_3	11.0, CH_3	11.0, CH_3	11.0, CH_3
5			15.0, CH_3	15.9, CH_3	15.7, CH_3	15.9, CH_3
*O*Bz-8 *CO*	166.5, C					
1	130.6, C					
2,6	129.8, CH					
3,5	128.9, CH					
4	133.0, CH					
*O*Nic *CO*			164.5, C			n.d.[c]
2			150.1, CH			150.9, CH
3			126.2, CH			128.0, CH
4			137.1, CH			137.5, CH
5			123.5, CH			123.8, CH
6			153.5, CH			153.5, CH

DOI: 10.1021/acs.jnatprod.6b00260
J. Nat. Prod. XXXX, XXX, XXX−XXX

Table 4. continued

[c]n.d. not detected.

Evaluation of the NOESY spectrum of **2** led to the conclusion that its configuration is the same as that of **1**. Diagnostic nuclear Overhauser effects were detected between H-4/H-3, H-4/H-1b, H-4/H-2, H-4/H-14, H-4/H-17a, H-3/OAc-5, and H-11/H-18, which proved the α-orientation of these protons. Moreover, the cross-peaks between H-5/H-12 and H-12/H-20 supported the β-orientation of H-5, H-12, and H-20. The structure of falcatin B (**2**) was elucidated therefore as 5α,10,14β,15β-*O*-tetraacetyl-3β-*O*-propanoyl-10,18-dihydromyrsinol.

Compound **3** was isolated as a colorless, amorphous solid with $[\alpha]^{28}_{D}$ +13 (*c* 0.1, $CHCl_3$). Its HRESIMS displayed a pseudomolecular ion peak at *m*/*z* 643.2756 $[M + Na]^+$, indicating a molecular composition of $C_{32}H_{44}O_{12}$. The ^1H NMR and JMOD spectra of **3** revealed four acetate and one isobutanoate group (Tables 1 and 2). Additionally, the spectra exhibited resonances closely related to those of **1** and **2**. ^1H and ^{13}C NMR assignments of **3**, determined by analysis of the $^1H-^1H$ COSY, HSQC, and HMBC spectra, clearly showed that compounds **1**−**3** are based on the same parent system and differ only in the substitution at C-3. In the case of **3**, an isobutanoate group can be found in this position, and its location was corroborated by the HMBC cross-peak between δ_H 5.39 (H-3) and the carbon signal at δ_C 176.6 (isobutanoyl CO). Comparison of the NOESY spectra of **2** and **3** indicated the same configuration for **3** and **2**. Therefore, falcatin C (**3**) was elucidated as 5α,10,14β,15β-*O*-tetraacetyl-3β-*O*-isobutyryl-10,18-dihydromyrsinol.

Compound **4** was obtained as an amorphous solid with $[\alpha]^{25}_{D}$ +16 (*c* 0.1, $CHCl_3$). It gave the molecular formula $C_{38}H_{48}O_{12}$, as determined from the HRESIMS by the protonated molecular ion peak at *m*/*z* 697.3256 $[M + H]^+$ (calcd for $C_{38}H_{49}O_{12}$, 697.3224). Apart from the signals for the benzoyl group, the main difference between **4** and **3** was the transposition of the locations of the keto group (at C-7 in **3** and C-14 in **4**) and an ester group (at C-14 in **3** and C-7 in **4**) (Tables 1 and 2). In addition, the chemical shift values of C-10 (δ_C 79.3) and C-13 (δ_C 84.6) suggested a rearranged tetrahydrofuran ring in the structure due to the ether bridge between C-10 and C-13 in **4**.[30−32] In compound **4**, the OH-17 group was esterified with an isobutanoic acid, as indicated by the HMBC cross-peaks between the carbon signal at δ_C 176.5 (*i*Bu CO) and H-17. The locations of the acyl groups at C-3, C-5, and C-7 were determined by the HMBC correlations of H-3, H-5, and H-7 to the corresponding carbonyl carbons of the acyl groups. The remaining acetoxy group was attached of necessity at C-15. The myrsinol-type diterpene skeleton of **4** implied the same *trans*-fusion of the three rings as those of compounds **1**−**3**. The NOESY correlations of H-2/H-3, H-3/H-4, and H-4/H_2-17 suggested that H-3, H-4, and H-17 are α-oriented. Correlations of H-5/H-12 and H-12/H_3-18 proved the β-orientation of H-5, H-12, and H_3-18, while NOEs between H-19/H-11 and H-20/H-17/H-1a/H-4 confirmed the α-orientation of these protons. Thus, compound **4** (falcatin D) was elucidated as 7β,15β-*O*-diacetyl-5α-*O*-benzoyl-17α-*O*-isobutanoyl-3β-*O*-propanoyl-10,13-epoxy-10,18-dihydromyrsinol.

The molecular formula for compound **5** was determined as $C_{37}H_{46}O_{12}$ on the basis of the HRESIMS [*m*/*z* 683.3092 $[M + H]^+$ (calcd for $C_{37}H_{47}O_{12}$, 683.3068)]. Comparing the chemical shifts for the skeletal carbons in **5** with those of compound **4**, the close similarity implied that compounds **4** and **5** possess the same 10,13-epoxy-10,18-dihydromyrsinol framework (Tables 1 and 2). Following the same NMR procedures used for **4**, the locations of the acyloxy groups in **5** and the configuration of the compound were determined by analysis of the HMBC and NOESY spectra. HMBC cross-peaks revealed acetoxy groups at C-7, C-15, and C-17, the isobutyryloxy group at C-3, and the benzoyloxy group at C-5, respectively. NOESY correlations of H-2/H-3, H-3/H-4, H-4/H_2-17, H_2-17/H-7, H-5/H-12, H-12/H_3-18, H-11/H_3-19, and H_2-17/H_3-20 allowed the stereochemical features to be assigned, which were identical with those of compound **4**. The structure of falcatin E was elucidated therefore as 7β,15β,17α-*O*-triacetyl-5α-*O*-benzoyl-3β-*O*-isobutyryl-10,13-epoxy-10,18-dihydromyrsinol.

Compound **6** was obtained as an amorphous solid with $[\alpha]^{25}_{D}$ +2 (*c* 0.1, $CHCl_3$). It exhibited a molecular formula of $C_{37}H_{48}O_{11}$ based on the HRESIMS [*m*/*z* 691.3125 $[M + Na]^+$ (calcd for $C_{37}H_{48}O_{11}Na$, 691.3094)]. The ^1H and ^{13}C NMR spectra of compound **6** were similar to those of **4** and **5** (Tables 1 and 2). For compound **6**, one acetoxy group, two isobutyryloxy units, and one benzoyloxy group were evident from its 1D NMR spectra (Table 1). The position of the acyloxy groups and the configuration of **6** were determined using HMBC and NOESY experiments. Nuclear Overhauser effects indicated that H-2, H-3, H-4, H-7, H_2-17, and H_3-20 are α-oriented and H-5, H-12, and the epoxy bridge are β-oriented. The differences between **6** and **5** were the presence of an isobutyroyl group at C-17 and a hydroxy group at C-15 instead of two acetyl groups at these positions. Therefore, compound **6** (falcatin F) was elucidated as 7β-*O*-acetyl-5α-*O*-benzoyl-15β-hydroxy-3β,17-*O*-diisobutyryl-10,13-epoxy-10,18-dihydromyrsinol.

The molecular formula $C_{40}H_{44}O_{13}$ of falcatin G (**7**) was assigned according to the HRESIMS at *m*/*z* 775.2986 $[M + H]^+$ (calcd for $C_{42}H_{47}O_{14}$, 775.2966). From the ^1H and ^{13}C NMR spectra, three acetoxy and two benzoyloxy groups were evident (Tables 3 and 4). The remaining 20 resonances in the ^{13}C NMR spectrum suggested a cyclomyrsinol-type diterpene skeleton for **7**. The characteristic cyclobutane ring, which is built with incorporation of one of the geminal dimethyl groups (C-19) besides C-9, C-10, and C-11 of the myrsinane skeleton, can be characterized by two methines [δ_C 29.8−30.7 (C-9), 41.1−41.5 (C-11)], one methylene [δ_C 34.6−37.1 (C-19)], and one O-substituted quaternary carbon [δ_C 77.5−77.8 (C-10)], due to the connection of an ester and a methyl group (C-18) in this position.[25,28,29]

The substitution pattern of compound **7** was determined using HMBC and NOESY experiments. The HMBC correlations of H-3, H-5, H-8, and H-14 to the corresponding carbonyl carbons revealed that the two acetoxy and two benzoyloxy groups are attached at C-3, C-5 and C-8, C-14, respectively. The remaining acetoxy groups were placed at C-10 and C-15. NOESY correlations observed for H-2/H-3, H-3/H-4, H-4/H-14, H-8/H-9, H-9/H_3-18, H-11/H-18, H-11/H-17, and H-5/H-12 suggested that the H-3, H-8, H-11, H-14, H-17, and H_3-18 are α-oriented and H-5 and H-12 are β-oriented. These assignments were consistent with the configurations of reported cyclomyrsinol diterpenes.[25,28,29] Therefore, compound **7** (falcatin G) was identified as 3β,10β,14β,15β-*O*-tetraacetyl-5α,8α-*O*-dibenzoylcyclomyrsinol.

DOI: 10.1021/acs.jnatprod.6b00260
J. Nat. Prod. XXXX, XXX, XXX−XXX

The ^{1}H and ^{13}C NMR spectra of compounds **8** and **9** were similar to those of falcatin G (**7**) (Tables 3 and 4). Chemical shift values for the 20 skeletal carbons were close to those of 3,5,8,10,14,15-*O*-hexaacylcyclomyrsinol, which implied that these compounds are polyesters of the same parent alcohol. For compound **8**, five acetoxy and one isobutyryloxy group were evident from its ^{13}C and ^{1}H NMR spectra. HMBC and NOESY experiments allowed the determination of the positions of the acyloxy groups and the relative configuration of **8** (Figure 3).

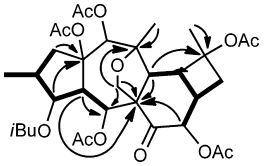

Figure 3. Selected ^{1}H−^{1}H COSY (bold) and HMBC (C→H) correlations for **8**.

NOESY correlations demonstrated that H-2, H-3, H-4, H-8, H-9, H-11, H-14, and H_2-17 are α-oriented and H-5, H-12, and H_3-20 are β-oriented. The two differences between **9** and **8** were that the C-3 isobutyryl and C-8 benzoyl groups in **8** were replaced by nicotinyl (C-3) and 2-methylbutyryl (C-8) groups in **9**. Therefore, compounds **8** and **9** were elucidated as 5α,8β,10β,14β,15β-*O*-pentaacetyl-3β-*O*-isobutyrylcyclomyrsinol (**8**) and 5α,10β,14β,15β-*O*-tetraacetyl-3β-isobutyryl-8β-*O*-(2-methylbutyryl)-3β-*O*-nicotinylcyclomyrsinol (**9**) and were named falcatins H and I, respectively.

Analysis of the ^{1}H and ^{13}C NMR data (Tables 3−6) of compounds **10**−**15** revealed all compounds to be based on a cyclomyrsinane skeleton in a similar manner to **8** and **9**, but having a hydroxy or acyloxy group substituent at C-2, as indicated by the carbon signals at $\delta_{C\text{-}2}$ 75.3−85.0 ppm. After defining the skeleton by ^{1}H−^{1}H COSY and HSQC measurements, HMBC and NOESY experiments were performed to determine the locations of the acyl groups and the configurations. For compound **10**, four acetoxy groups at C-5, C-10, C-14, and C-15, a propionyloxy group at C-3, a 2-methylbutyryloxy group at C-8, and a hydroxy group at C-2 were elucidated. The only difference found between **11** and **10** was that the C-3 propionyloxy group in **10** was replaced by an isobutyryloxy group in **11**. Compound **12** differs from **11** by the substitution at C-2. In the case of **12**, a nicotinyloxy group was determined as being present instead of a hydroxy group in **11**, as indicated by the chemical shift values of C-2 (**11**: 75.5 ppm, **12**: 85.0 ppm).

The only structural difference between **12** and **13** was the presence of an isobutyryloxy group at C-8 in **13** instead of the 2-methylbutyryloxy group in **12**. Compound **14** differed from **13** also in that a propionyloxy group was determined at C-3 instead of the isobutyryloxy group found in **13**. Compound **15** was a close analogue of **10**, differing only in the substituent at C-2 (hydroxy in **10** and benzoyloxy in **15**).

NOE effects observed between H-3/H-4, H-4/H-14, H-4/H_3-16, H-4/H-17a, H-11/H-17b, H-14/H-1α, H-8/H-9, H-9/H-18, H-18/H-11, and H-5/H-12 in compounds **10**−**15** revealed that these compounds have the same configuration, namely, H-3, H-4, H-9, H-11, H-14, and H_2-17 in an α-orientation and H-5 and H-12 β-oriented. All of the above evidence confirmed the structures of these compounds as depicted in structural formulas **10**−**15**, and the compounds were named falcatins J−O, respectively.

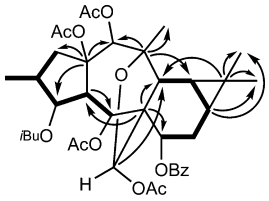

Figure 4. Selected ^{1}H−^{1}H COSY (bold) and HMBC (C→H) correlations for **16**.

The ^{1}H and ^{13}C NMR spectra of compounds **16**−**18** were very similar (Tables 5−7). From the NMR spectra, a hemiacetal moiety between C-13 and C-6 could be elucidated with regard to the oxymethine signals at δ_H 6.36−6.49 s and δ_C 97.1 (17-CH). In the case of all three compounds, six acyl groups were identified. The ^{1}H NMR and ^{1}H−^{1}H COSY spectra revealed the structural elements −CH_2−CH(CH_3)−CHR−CH−CHR− (C-1−C-2(C-16)−C-3−C-4−C-5) and −CHR−CH_2−CH−CH−CH− (C-7−C-12). The connection of these partial structural parts was carried out with the use of HMBC correlations. Diagnostic HMBC cross-peaks between C-17/H-5, C-17/H-7, C-17/H-12, C-10/H-18, C-10/H-19, C-10/H-12, C-9/H-18, C-9/H-19, and C-9/H-11 led to the conclusion that these compounds are premyrsinane derivatives. For compound **16**, four acetoxy, one isobutyryloxy, and one benzoyloxy group were identified from its ^{13}C and ^{1}H NMR spectra. The locations of the ester groups were established from the HMBC spectra, with the acetoxy groups present at C-5, C-14, C-15, and C-17, an isobutyryloxy group at C-3, and a benzoyloxy group at C-7 (Figure 4).

In the case of **17**, in addition to acetyl substituents at C-5, C-15, and C-17 and the isobutanoyl group at C-3, a nicotinyl group and a benzoyl group were determined at C-8 and C-14, respectively. Compound **18** was found to possess a propionyloxy moiety at C-3 instead of the isobutyryloxy moiety in **17** (Tables 5−7). A careful comparison of the NOESY spectra of **16**−**18** indicated the same configuration for all three compounds. A strong NOESY cross-peak between H-4/H-17 proved the α-orientation of the C-17 methine proton. Moreover, NOE correlations observed for H-2/H-3, H-3/H-4, H-4/H-14, H-7/H-8a, H-8a/H-9, H-9/H-11, H-5/H-12, and H-12/H_3-20 indicated that H-2, H-3, H-4, H-7, H-9, H-11, and H-14 are α-oriented, while H-5, H-12, and H_3-20 are oriented in a β-manner. Therefore, compounds **16**−**18** (falcatins P−R) were elucidated as 5α,14β,15β,17-*O*-tetraacetyl-7β-*O*-benzoyl-3α-*O*-isobutyryl-premyrsinol (**16**), 5α,15β,17-*O*-triacetyl-14β-benzoyl-3α-*O*-isobutyryl-7β-*O*-nicotinylpremyrsinol (**17**), and 5α,15β,17-*O*-triacetyl-14β-benzoyl-7β-*O*-nicotinyl-3α-*O*-propionylpremyrsinol (**18**), respectively.

The molecular formula, $C_{41}H_{49}NO_{12}$, was determined for compound **19** by the HRESIMS at m/z 748.3373 $[M + H]^+$ (calcd for $C_{41}H_{50}NO_{12}$, 748.3333). Analysis of its ^{13}C NMR spectrum (Table 6) revealed the presence of five ester carbonyls (δ_C 164.7, 164.9, 170.0, 170.6, and 176.0), which could be assigned to a nicotinate, a benzoate, two acetate, and one isobutanoate unit, respectively, based on diagnostic resonances in the ^{1}H and ^{13}C NMR spectra (Tables 6 and 7). Analysis of the ^{1}H−^{1}H COSY spectrum allowed the identification of the two spin systems, −CH_2−CH(CH_3)−CH(R)−CH−CH(R)− (A) and −CH(R)−CH_2−CH−CH−CH− (B), and an isolated *O*-substituted methylene (−CH_2−OR). HMBC cross-peaks between C-6 and H-5, H-17a, H-12, H-4, and H-8, between C-7 and H-5, H-17, and H-8, and between C-10 and H-7, H-12, H-

DOI: 10.1021/acs.jnatprod.6b00260
J. Nat. Prod. XXXX, XXX, XXX−XXX

Table 5. ^{1}H NMR Data (δ_H) of Compounds 13−17 ($CDCl_3$, 500 MHz[a] or 600 MHz[b])

position	13[a]	14[a]	15[a]	16[b]	17[a]
1α	3.84, d (16.8)	4.22, d (16.9)	4.15, d (16.8)	2.62, m	2.78, dd (16.1, 10.2)
1β	2.84, d (16.7)	2.42, d (16.7)	2.44, d (16.7)	2.39, m	2.67, dd (16.1, 10.0)
2				2.02, m	2.15, m
3	5.61, d (4.4)	5.57, d (5.5)	5.60, d (5.4)	5.02, t (3.6)	5.12, t (3.8)
4	3.21, dd (10.8, 4.4)	3.08, dd (10.8, 5.6)	3.08, dd (10.8, 5.4)	3.02, dd (10.8, 3.6)	3.17, dd (10.7, 3.7)
5	5.92, d (10.8)	5.94, d (10.7)	5.90, d (10.7)	5.77, d (10.8)	5.88, d (10.6)
7				5.31, dd (10.8, 3.1)	5.42, dd (10.6, 3.5)
8	5.27, d (6.6)	5.28, d (6.6)	5.27, d (6.6)	2.02, m; 1.55, m	2.15, m; 1.70 m
9	2.76, m	2.76, m	2.74, m	0.91, m	1.02, m
11	2.52, m	2.47, m	2.46, m	0.74, m	0.89, t (7.0)
12	4.04, d (12.3)	3.97, d (12.2)	3.97, d (12.2)	2.66, m	2.93, d (7.0)
14	5.05, s	5.03, s	5.03, s	4.97, s	5.30, s
16	1.80, s	1.83, s	1.80, s	0.69, d (6.6)	0.76, d (6.8)
17	4.27, d (9.8)	4.26, d (9.8)	4.27, d (9.8)	6.36, s	6.48, s
	3.64, d (9.8)	3.62, d (9.9)	3.61, d (9.8)		
18	1.66, s	1.64, s	1.64, s	1.13, s	1.28, s
19	2.52, m	2.52, m	2.52, m	1.13, s	1.18, s
20	1.22, s	1.20, s	1.20, s	1.29, s	1.37, s
*O*Prop-3					
2		2.21, m, 2.16, dq (16.5, 7.5)	2.17, m		
3		1.06, t (7.5)	1.04, t (7.5)		
*Oi*Bu-3					
2	2.40, sept (7.0)			2.43, m	2.49, sept (7.0)
3	1.06, d (6.9)			1.07, d (6.6)	1.11, d (7.0)
4	1.00, d (7.1)			1.05, d (6.6)	1.09, d (7.0)
*O*Ac-5	1.96, s	1.94, s	1.94, s	1.23, s	1.39, s
*O*Ac-10	2.10, s	2.07, s	2.08, s		
*O*Ac-14	2.12, s	2.09, s	2.11, s	1.98, s	
*O*Ac-15	2.16, s	2.05, s	2.05, s	2.04, s	2.08, s
*O*Ac-17				2.13, s	2.21, s
*Oi*Bu-8					
2	2.76, m	2.76, m			
3	1.26, d (6.8)	1.24, d (7.0)			
4	1.23, d (7.2)	1.28, d (6.8)			
*O*MeBu-8					
2			2.52, m		
3			1.29, d (7.0)		
4			0.88, t (7.0)		
5			1.23, d (7.1)		
*O*Nic					
2	9.06, s	9.03, s			9.15, s
4	8.15, d (7.9)	8.18, d (8.0)			8.23, d (7.9)
5	7.36, dd (8.0, 5.0)	7.39, dd (8.1, 4.9)			7.38, dd (7.8, 4.9)
6	8.76, d (4.8)	8.76, d (4.8)			8.78, d (4.7)
*O*Bz					
2, 6			7.89, d (8.2)	7.88, d (7.8)	7.95, d (7.3)
3, 5			7.41, t (7.8)	7.34, t (7.6)	7.47, t (7.8)
4			7.53, t (7.4)	7.47, t (7.2)	7.59, t (7.4)

8, H_3-18, and H_3-19 indicated a premyrsinane skeleton without the ether functionality between C-17 and C-13. The locations of the ester groups were established from the HMBC correlations from δ_C 176.0 to δ_H 5.39 (H-3); δ_C 164.9 to δ_H 6.42 (H-5); δ_C 164.7 to δ_H 5.04 (H-17); and δ_C 170.0 to δ_H 5.01 (H-7) and indicated that isobutanoyl, benzoyl, nicotinyl, and acetyl groups occurred at C-3, C-5, C-7, and C-17, respectively. The chemical shift at $\delta_{C\text{-}15}$ 84.1 indicated clearly a hydroxy group at C-15, and the last acetyl group was placed at C-13. NOESY experiments led to the assignment of the configuration of the molecule. Starting from the α-orientation of H-4, cross-peaks between H-4/H-3, H-4/H-2, H-4/H-17a, H-4/H_3-20, and H-20/H-11 demonstrated the α-orientation of these protons. The NOE effects observed between H-5/H-12 and H-5/OH-15 indicated the β-orientation of H-5, H-12, and OH-15. Consequently, the data obtained supported the proposed structure of **19** (falcatin S) as 7β,13β-*O*-diacetyl-5α-*O*-benzoyl-15β-hydroxy-3β-*O*-isobutanoyl-17α-*O*-nicotinylpremyrsinol.

Compound **20** was found to be identical in all of its characteristics, including the ^{1}H NMR and mass spectrometric data, with euphorprolitherin D, isolated earlier from *Euphorbia prolifera* by Zhang et al. in 2004.[33]

DOI: 10.1021/acs.jnatprod.6b00260
J. Nat. Prod. XXXX, XXX, XXX−XXX

Table 6. ^{13}C NMR Data (δ_C) of Compounds 13−19 ($CDCl_3$, 125 MHz[a] or 150 MHz[b])

position	13[a]	14[a]	15[a]	16[b]	17[a]	18[a]	19[a]
1	48.3, CH_2	48.8, CH_2	49.1, CH_2	44.3, CH_2	44.3, CH_2	44.2, CH_2	42.9, CH_2
2	84.2, C	84.2, C	83.6, C	35.9, CH	36.2, CH	35.7, CH	37.1, CH
3	78.1, CH	78.4, CH	78.2, CH	76.4, CH	76.6, CH	76.5, CH	77.9, CH
4	47.0, CH	48.6, CH	48.6, CH	53.2, CH	53.4, CH	53.5, CH	50.5, CH
5	68.4, CH	68.9, CH	68.9, CH	67.1, CH	67.4, CH	67.4, CH	69.9, CH
6	62.0, C	62.2, C	62.2, C	55.9, C	56.1, C	55.6, C	48.1, C
7	204.3, C	204.5, C	204.6, C	72.6, CH	72.9, CH	73.1, CH	70.5, CH
8	70.8, CH	70.9, CH	70.9, CH	25.6, CH_2	22.9, CH_2	22.9, CH_2	22.2, CH_2
9	29.9, CH	30.0, CH	30.1, CH	23.6, CH	23.4, CH	23.2, CH	23.8, CH
10	77.5, C	77.5, C	77.6, C	19.1, C	19.1, C	19.3, C	18.3, C
11	41.5, CH	41.3, CH	41.3, CH	18.5, CH	18.5, CH	18.6, CH	18.3, CH
12	41.3, CH	41.5, CH	41.5, CH	38.1, CH	37.8, CH	37.9, CH	35.3, CH
13	89.1, C	88.7, C	88.8, C	87.8, C	88.6, C	88.1, C	85.5, C
14	81.5, CH	80.8, CH	80.9, CH	79.7, CH	80.4, CH	80.2, CH	204.0, C
15	88.5, C	89.3, C	89.3, C	89.8, C	89.8, C	89.8, C	84.1, C
16	24.7, CH_3	25.6, CH_3	25.5, CH_3	14.2, CH_3	14.6, CH_3	14.4, CH_3	13.7, CH_3
17	67.1, CH_2	67.0, CH_2	67.0, CH_2	97.1, CH	97.3, CH	97.1, CH	63.6, CH_2
18	24.4, CH_3	24.6, CH_3	24.6, CH_3	15.8, CH_3	16.6, CH_3	16.1, CH_3	14.8, CH_3
19	34.6, CH_2	34.6, CH_2	34.7, CH_2	28.1, CH_3	28.3, CH_3	28.1, CH_3	29.4, CH_3
20	22.2, CH_3	22.3, CH_3	22.2, CH_3	24.8, CH_3	25.1, CH_3	25.0, CH_3	24.9, CH_3
*O*Prop-3 1		173.0, C	173.0, C			174.0, C	
2		27.3, CH_2	27.3, CH_2			27.6, CH_2	
3		8.6, CH_3	8.5, CH_3			9.0, CH_3	
*O*iBu-3 1	175.3, C			176.8, C			176.0, C
2	34.0, CH			34.3, CH			34.1, CH
3	18.2, CH_3			19.5, CH_3			19.2, CH_3
4	18.9, CH_3			18.6, CH_3			18.4, CH_3
*O*Ac-5	169.7, C	169.9, C	170.2, C	169.2, C	168.9, C	169.1, C	
	20.8, CH_3	20.8, CH_3	20.3, CH_3	21.2, CH_3	21.5, CH_3	21.4, CH_3	
*O*Ac-7							170.0, C
							21.3, CH_3
*O*Ac-10	168.7, C	168.7, C	168.8, C				
	21.5, CH_3	21.2, CH_3	21.5, CH_3				
*O*Ac-13							170.6, C
							21.3, CH_3
*O*Ac-14	170.2, C	170.1, C	170.0, C	170.2, C			
	21.2, CH_3	21.2, CH_3	21.3, CH_3	21.0, CH_3			
*O*Ac-15	168.1, C	168.1, C	168.5, C	168.4, C	167.9, C	167.9, C	
	22.9, CH_3	22.3, CH_3	20.9, CH_3	23.0, CH_3	23.0, CH_3	22.9, CH_3	
*O*Ac-17				170.0, C	170.0, C	169.8, C	
				21.4, CH_3	21.6, CH_3	21.4, CH_3	
*O*iBu 1	175.0, C	174.9, C			176.5, C		
2	34.3, CH	34.4, CH			34.5, CH		
3	18.4, CH_3	20.3, CH_3			19.1, CH_3		
4	20.3, CH_3	18.5, CH_3			18.8, CH_3		
*O*MeBu-8 1			174.9, C				
2			34.9, CH				
3			18.5, CH_2				
4			14.1, CH_3				
5			20.3, CH_3				
*O*Bz CO			164.7, C	166.1, C	165.3, C	165.5, C	164.9, C
1			129.4, C	129.9, C	130.0, C	129.6, C	129.3, C
2, 6			128.3, CH	128.3, CH	128.6, CH	128.4, CH	127.9, CH
3, 5			133.0, CH	133.1, CH	133.3, CH	133.1, CH	132.7, CH
4			130.5, CH	130.3, CH	129.7, CH	129.4, CH	129.4, CH
*O*Nic 1	163.4, C	163.4, C			164.4, C	164.8, C	164.7, C
2	150.7, CH	150.4, CH			151.3, CH	150.7, CH	150.4, CH
3	126.2, CH	126.6, CH			124.8, CH	128.3, CH	125.1, CH
4	137.0, CH	137.0, CH			137.5, CH	137.2, CH	136.1, CH
5	123.2, CH	123.4, CH			123.3, CH	123.2, CH	123.0, CH
6	153.4, CH	153.4, CH			153.8, CH	153.6, CH	153.0, CH

DOI: 10.1021/acs.jnatprod.6b00260
J. Nat. Prod. XXXX, XXX, XXX−XXX

Table 7. ^{1}H NMR Data (δ_H) of Compounds 18 and 19 ($CDCl_3$, 500 MHz)

position	18	19
1α	2.81, dd (16.1, 9.6)	3.19, dd (13.6, 7.8)
1β	2.63, dd (16.1, 9.6)	1.65, m
2	2.20, m	1.87, m
3	5.13, t (3.9)	5.39, d (3.5)
4	3.15, dd (10.6, 3.7)	2.44, dd (11.6, 3.5)
5	5.88, d (10.6)	6.42, d (11.6)
7	5.43, dd (10.8, 3.3)	5.01, m
8	2.12, m	2,16, m
	1.67, m	1.93, m
9	1.04, m	0.78, m
11	0.88, t (7.7)	0.78, m
12	2.91, d (7.2)	3.61, d (6.2)
14	5.29, s	
16	0.76, d (6.8)	0.86, d (6.5)
17a	6.48, s	5.04, d (11.6)
17b		4.56, d (11.6)
18	1.28, s	1.08, s
19	1.18, s	0.98, s
20	1.36, s	1.78, s
*O*Ac-5	1.38, s	1.94, s
OAc-7		2.16, s
OAc-13		2.14, s
*O*Ac-15	2.07, s	
*O*Ac-17	2.23, s	
*O*Prop-3		
2	2.32, m,	
	2.22, dq (16.5, 7.6)	
3	1.07, t (7.6)	
*O*i*B*u		
2		2.49, sept (7.0)
3		1.14, d (7.0)
4		0.96, d (7.0)
*O*Bz		
2, 6	7.95, d (7.4)	7.70, d (7.4)
3, 5	7.47, t (7.8)	7.03, t (7.7)
4	7.59, t (7.4)	7.16, t (7.3)
*O*Nic		
2	9.15, s	8.84, d (1.3)
4	8.24, d (7.6)	7.61, dt (7.9, 1.3)
5	7.39, dd (7.6, 4.9)	7.00, dd (8.0, 4.7)
6	8.78, d (4.9)	8.54, dd (4.7, 1.3)
15-OH		4.38, s

Effects of the Investigated Compounds on GIRK and hERG Potassium Channels. In order to study the possible potassium channel-blocking capability of the investigated compounds, screening of the isolated diterpenes with different skeletons and substitution patterns was performed on a GIRK channel expressing cell line. Myrsinane, premyrsinane, and cyclomyrsinane diterpenes substituted with hydroxy, acetyl, propanoyl, isobutanoyl, 2-methylbutanoyl, *n*-hexanoyl, benzoyl, and nicotinyl ester groups were included in the bioassay. Compounds were screened at two concentrations (1 and 10 μM) on two to three cells.

Thirteen of the tested compounds (**1**–**3**, **8**, **9**, **12**, **14**, **15**, and **21**–**24**) were found to possess blocking activity (i.e., at least 60% decrease in the current at 10 μM concentration) on GIRK channels. All compounds were also tested against the HEK-hERG (human embryonic kidney cells) cell line, and the

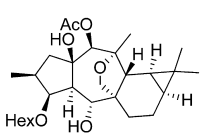

21

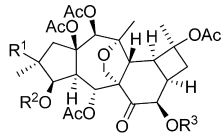

	R^1	R^2	R^3
22	OBz	*i*Bu	MeBu
23	OBz	*i*Bu	*i*Bu
24	H	Prop	*i*Bu

selectivity of their GIRK blocking effect was evaluated with these experiments. Selectivity studies were performed at three concentrations (3, 10, and 30 μM) on two or three cells. Five out of the 13 compounds, falcatins A–C (**1**–**3**), falcatin H (**8**), and falcatin I (**9**), which were potent for GIRK channels, exerted low inhibitory effects on the hERG channel (i.e., a maximum 20% decrease in the current at 10 μM concentration). Results of the GIRK screening and the selectivity investigations on hERG are shown in Table 8.

Table 8. GIRK- and hERG-Inhibitory Effects of Compounds Isolated from *E. falcata*

	inhibition (%)				
	GIRK		hERG		
compound	1 μM	10 μM	3 μM	10 μM	30 μM
1	43	83	9	20	39
2	24	62	5	13	18
3	34	69	0	4	16
4	21	47	11	24	40
5	26	61	13	24	43
6	21	54	20	33	46
8	28	61	8	16	23
9	31	72	4	14	25
10	11	24	8	20	33
11	14	26	12	22	32
12	23	69	20	54	82
13	8	57	8	19	30
14	35	65	11	22	42
15	20	64	16	31	52
17	18	37	48	68	78
19	28	48	14	29	53
20	19	54	12	21	45
21	30	69	19	40	55
22	26	70	14	30	40
23	33	77	14	24	53
24	30	70	0	23	33

Compounds with a myrsinane skeleton and with a carbonyl function at C-7 (**1**–**3**) were found to be highly active and selective inhibitors. In addition, esters of 2-deoxycyclomyrsinane with an aliphatic ester group at C-8 (**8** and **9**) were also found to have selective ion channel activity. These compounds showing GIRK selectivity were subjected to further investigations. The dose–response curves of these five compounds on the GIRK channel were determined in detailed experiments where the effect of the compounds was tested at four concentrations on at least five cells. Dose–response curves and IC_{50} values of these compounds are shown in Figure 5.

Falcatin A (**1**) was the most promising agent, with an IC_{50} value of 2.5 ± 0.2 μM. The IC_{50} values of falcatins C (**3**) and I (**9**) were very similar (4.7 ± 0.3 and 4.9 ± 0.2 μM, respectively). In

DOI: 10.1021/acs.jnatprod.6b00260
J. Nat. Prod. XXXX, XXX, XXX–XXX

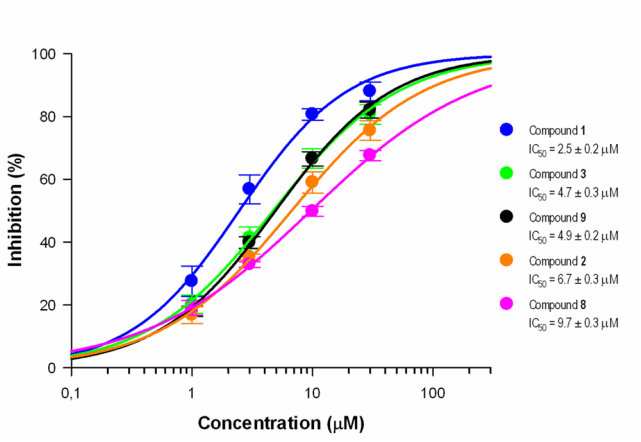

Figure 5. Dose−response curves of compounds **1**−**3**, **8**, and **9** on GIRK channel inhibitory activity.

turn, the IC_{50} value of falcatin B (**2**) was 6.7 ± 0.3 μM, whereas that of falcatin H (**8**) was determined to be 9.7 ± 0.3 μM. Sample current curves and time course of the hERG and GIRK current amplitude during the application of different concentrations of the most effective compound (falcatin A, **1**) are shown in Figure 6.

CONCLUSIONS

Nineteen new diterpenes, falcatins A−S (**1**−**19**), and the known compound euphorprolitherin D (**20**) were isolated from the whole plants of *E. falcata*. The new compounds were identified as tetra-, penta-, hexa-, and heptaesters of the myrsinane, premyrsinane, and cyclomyrsinane polyols acylated with acetyl, propanoyl, isobutanoyl, 2-methylbutanoyl, benzoyl, and nicotinyl acids. Falcatins D−F (**4**−**6**) contain a rare 10,13-epoxy functionality in their myrsinane structure. Moreover, falcatins L−O (**12**−**15**) are substituted with an ester group, and falcatins J and K (**10** and **11**) possess a hydroxy group at C-2. This subclass of the cyclomyrsinanes has been found only in *E. falcata* so far. Biogenetically, naturally occurring myrsinanes and cyclomyrsinanes can be derived from lathyranes through premyrsinanes by intramolecular cyclization.[34] Myrsinol-related diterpenes are specific to the genus *Euphorbia*; up to now more than 110 such compounds, including myrsinanes (n = 58), premyrsinanes (n = 39), and cyclomyrsinanes (n = 19), were isolated from 15 *Euphorbia* species (*E. aellenii*, *E. aleppica*, *E. boetica*, *E. cheiradenia*, *E. decipiens*, *E. falcata*, *E. kopetdaghi*, *E. macroclada*, *E. microsciadia*, *E. myrsinites*, *E. pithyusa* subsp. *cupanii*, *E. prolifera*, *E. splendida*, *E. seguieriana*, and *E. teheranica*).[22,35−39] Among them, the presence of all three types of myrsinanes has been reported only from *E. prolifera*, *E. seguieriana*, and *E. falcata*. The richest source of diterpenes seems to be *E. prolifera*; to date, 46 such compounds were isolated from the plant, and tigliane- and lathyrane-type diterpenes were also identified along with myrsinols.[40,41] Moreover, in our study three compounds (**4**−**6**) with a rearranged tetrahydrofuran ring were also isolated from *E. falcata*. Previously this type of diterpene was detected in only two species (*E. decipiens* and *E. cheiradenia*).[30−32]

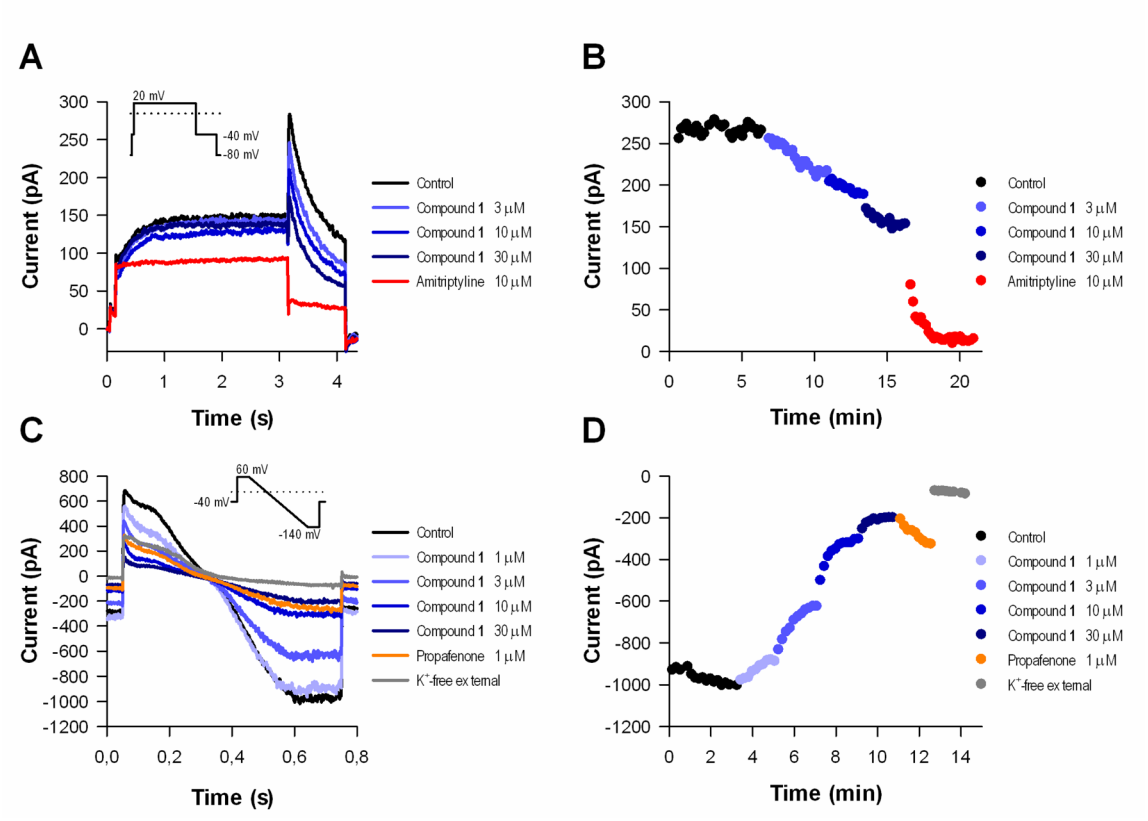

Figure 6. Effects of compound **1** on the hERG and GIRK current. (A) Representative hERG current curves recorded during the application of 3, 10, and 30 μM compound **1**. The inset shows the applied hERG voltage protocol. (B) Time-course of the hERG current amplitude. (C) Typical GIRK current curves obtained after the application of 1, 3, 10, and 30 μM compound **1**. The inset shows the applied GIRK voltage protocol. (D) Illustrative time series showing the GIRK inward current values.

DOI: 10.1021/acs.jnatprod.6b00260
J. Nat. Prod. XXXX, XXX, XXX−XXX

Myrsinane-related diterpenes are interesting targets of natural product based drug discovery programs. Recently, their antiangiogenic, immunomodulatory, immunosuppressive, neuroprotective, LPS-induced NO production inhibitory, MDR reversal, cytotoxic, DNA-damaging, antipyretic-analgesic, prolyl endopeptidase inhibitory, and urease inhibitory activities have been reported.[25,35−38,42−46] This is the first time that selective GIRK channel inhibitory activity of natural diterpenes has been investigated.

In the present study, myrsinane, cyclomyrsinane, and premyrsinane diterpenes were studied on stable transfected HEK-hERG (Kv11.1) and HEK-GIRK1/4 (Kir3.1 and Kir3.4) cells. Blocking activity on the GIRK channel was exerted by 13 compounds (**1**−**3**, **8**, **9**, **12**, **14**, **15**, and **21**−**24**) (61−83% at 10 μM), and, among them, five [falcatins A−C (**1**−**3**), falcatin H (**8**), and falcatin I (**9**)] showed low potencies on hERG channels (4−20% at 10 μM). These compounds with selective activities on GIRK channels are potential lead compounds for the treatment of atrial fibrillation. The electrophysiological screening of structurally diverse diterpenes did not permit a detailed structure−activity relationship determination, but it was observed that the most promising compounds, **1**−**3**, are myrsinanes with a carbonyl function at C-7, an ether bridge between C-17 and C-13, and no epoxy functionality between C-10 and C-13. Another group of promising GIRK ion channel inhibitory compounds was established as 2-deoxycyclomyrsinanes with an aliphatic ester at C-8 (compounds **8** and **9**).

EXPERIMENTAL SECTION

General Experimental Procedures. Optical rotations were measured in $CHCl_3$ using a PerkinElmer 341 polarimeter. NMR spectra were recorded in $CDCl_3$ on a Bruker Avance DRX 500 spectrometer at 500 MHz (^{1}H) and 125 MHz (^{13}C) and a Bruker Ultrashield Plus 600 spectrometer at 600 MHz (^{1}H) and 150 MHz (^{13}C), using the signals of deuterated solvents as references. Two-dimensional NMR data were acquired and processed with standard Bruker software. Gradient-enhanced versions of the experiments were used. High-resolution MS data were recorded on a Waters-Micromass Q-TOF Premier mass spectrometer equipped with an electrospray source. The resolution was over 1 ppm. The data were acquired and processed with MassLynx software. Column chromatography (CC) was carried out on polyamide (ICN); vacuum liquid chromatography (VLC) on silica gel G (15 μm, Merck); preparative thin-layer chromatography (preparative TLC) on silica gel 60 F_{254} and RP-18 F_{254} plates (Merck); rotation planar chromatography (RPC) on silica gel 60 GF_{254} with a Chromatotron instrument (Harrison Research); and reversed-phase HPLC on a LiChrospher RP-18 (5 μm, 250 × 4 mm, Merck) column with a Waters 600 instrument with detection at 254 nm.

Plant Material. *Euphorbia falcata* was collected in September 2008 in Mosonmagyaróvár (Hungary). The plant material was identified by one of the authors (G.P.). A voucher specimen (No. 775) has been deposited at the Herbarium of the Department of Pharmacognosy, University of Szeged, Szeged, Hungary.

Extraction and Isolation. The fresh plant material (20 kg), which was stored at −20 °C before processing, was crushed in a blender and then percolated with MeOH (178 L) at room temperature. The crude extract was concentrated in vacuo and subjected to solvent−solvent partitioning with $CHCl_3$ (30 L). On evaporation, an organic-phase residue of 344 g was obtained, which was chromatographed over a polyamide column (1100 g) with mixtures of H_2O−MeOH (4:1, 3:2, 2:3, and 1:4) as eluents. The fractions obtained with H_2O−MeOH (4:1 and 3:2) were combined and subjected to silica gel VLC, using a gradient system of cyclohexane−EtOAc−MeOH (from 8:2:0 to 0:0:1). The CC fractions were combined into six fractions according to the TLC monitoring (fractions 1−6). Fraction 3, eluted with cyclohexane−EtOAc (7:3), was separated by RPC with cyclohexane−CH_2Cl_2−MeOH of increasing polarity (from 8:2:0 to 60:50:3). Subfraction 3/3, eluted with cyclohexane−CH_2Cl_2−MeOH (60:30:2), was purified further by RP-VLC (MeOH−H_2O from 1:1 to 85:15) and finally by NP-TLC with $CHCl_3$−acetone (98:2) to yield falcatin P (**16**) (1.4 mg). Fraction 4, obtained with cyclohexane−EtOAc−MeOH (70:30:2), was further separated by RPC with a cyclohexane−CH_2Cl_2−MeOH (from 60:30:2 to 50:50:4) gradient system. Subfraction 4/3 eluted with cyclohexane−CH_2Cl_2−MeOH (60:40:3) was purified by NP-TLC with *n*-hexane−acetone (3:2), then by RP-HPLC with MeOH−H_2O (3:1) as eluent, at a flow rate of 0.5 mL/min, to afford falcatin G (**7**) (1.1 mg) at t_R 30.3 min. Fraction 5, obtained with cyclohexane−EtOAc−MeOH (70:30:2), was subjected to RPC, eluted with cyclohexane−CH_2Cl_2−MeOH mixtures of increasing polarity (from 70:20:1 to 5:5:1). Subfraction 5/3, eluted with cyclohexane−CH_2Cl_2−MeOH (60:30:2), was further separated on RP-VLC using a MeOH−H_2O (from 1:1 to 9:1) gradient system as eluent. Subfraction 5/3/2, eluted with MeOH−H_2O (1:1), was purified further by NP-TLC, with toluene−acetone (9:1) as developing system, to yield falcatin C (**3**) (46.3 mg). Subfraction 5/3/3, eluted with MeOH−H_2O (3:2), was separated by RP-TLC with MeOH−H_2O (9:1) to afford falcatin B (**2**) (3.3 mg). Subfraction 5/3/4, eluted with MeOH−H_2O (7:3), was purified by NP-TLC with toluene−acetone (4:1) to yield falcatin H (**8**) (6.3 mg) and falcatin O (**15**) (12.3 mg). Subfraction 5/3/5, eluted with MeOH−H_2O (7:3 and 8:2), was separated by NP-TLC with cyclohexane−CH_2Cl_2−MeOH (5:15:1), to yield falcatin K (**11**) (5.5 mg), falcatin F (**6**) (2.5 mg), and euphorprolitherin D (**20**) (2.9 mg). The compound observed at R_f 0.6 was further purified by RP-HPLC, eluted with MeOH−H_2O (7:3) at a flow rate of 1 mL/min, to afford falcatin D (**4**) (6.7 mg) (t_R 11.2 min). Fraction 6, eluted with cyclohexane−EtOAc−MeOH (20:10:1), was rechromatographed by NP-VLC with cyclohexane−EtOAc−MeOH (from 6:2:0 to 1:1:1). Subfraction 6/4, eluted with cyclohexane−EtOAc−MeOH (5:5:1), was further separated by RPC with cyclohexane−CH_2Cl_2−MeOH (from 5:15:0 to 15:45:15) as the eluent system. Subfractions yielded with mixtures of cyclohexane−CH_2Cl_2−MeOH (15:45:0.5, 15:45:1.5, and 15:45:3) were finally purified by RP-TLC with MeOH−H_2O (4:1), to yield falcatin A (**1**) (24.3 mg), falcatin Q (**17**) (4.4 mg), falcatin I (**9**) (6.1 mg), and falcatin L (**12**) (3.7 mg). Subfraction 6/5, eluted with cyclohexane−EtOAc−MeOH (1:1:1), was separated further by RP-VLC with a MeOH−H_2O (from 1:1 to 9:1) gradient system to afford falcatin S (**19**) (10.0 mg), falcatin N (**14**) (4.0 mg), falcatin E (**5**) (2.5 mg), falcatin J (**10**) (8.3 mg), and falcatin R (**18**) (2.7 mg). The subfraction obtained by RP-VLC with MeOH−H_2O (4:1) was purified by RP-HPLC with MeOH−H_2O (7:3), at a flow rate of 1.0 mL/min, to afford falcatin N (**14**) (11.1 mg) (t_R 15.4 min) and falcatin M (**13**) (36.5 mg) (t_R 19.2 min).

*Falcatin A (**1**):* amorphous solid; $[\alpha]^{25}_D$ −8 (*c* 0.2, $CHCl_3$); ^{1}H and ^{13}C NMR data, see Tables 1 and 2; HRESIMS *m*/*z* 677.2594 $[M + Na]^+$ (calcd for $C_{35}H_{42}O_{12}Na$, 677.2574), 672.3051 $[M + NH_4]^+$ (calcd for $C_{35}H_{46}NO_{12}$, 672.3020).

*Falcatin B (**2**):* amorphous solid; $[\alpha]^{28}_D$ +22 (*c* 0.1, $CHCl_3$); ^{1}H and ^{13}C NMR data, see Tables 1 and 2; HRESIMS *m*/*z* 629.2600 $[M + Na]^+$ (calcd for $C_{31}H_{42}O_{12}Na$, 629.2574), 624.3051 $[M + NH_4]^+$ (calcd for $C_{31}H_{46}NO_{12}$, 624.3020).

*Falcatin C (**3**):* amorphous solid; $[\alpha]^{28}_D$ +13 (*c* 0.1, $CHCl_3$); ^{1}H and ^{13}C NMR data, see Tables 1 and 2; HRESIMS *m*/*z* 643.2756 $[M + Na]^+$ (calcd for $C_{32}H_{44}O_{12}Na$, 643.2731), 638.3211 $[M + NH_4]^+$ (calcd for $C_{32}H_{48}NO_{12}$, 638.3177).

*Falcatin D (**4**):* amorphous solid; $[\alpha]^{25}_D$ +16 (*c* 0.1, $CHCl_3$); ^{1}H and ^{13}C NMR data, see Tables 1 and 2; HRESIMS *m*/*z* 697.3256 $[M + H]^+$ (calcd for $C_{38}H_{49}O_{12}$, 697.3224), 719.3070 $[M + Na]^+$ (calcd for $C_{38}H_{48}O_{12}Na$, 719.3044).

*Falcatin E (**5**):* amorphous solid; $[\alpha]^{25}_D$ +14 (*c* 0.2, $CHCl_3$); ^{1}H and ^{13}C NMR data, see Tables 1 and 2; HRESIMS *m*/*z* 683.3092 $[M + H]^+$ (calcd for $C_{37}H_{47}O_{12}$, 683.3068), 705.2907 $[M + Na]^+$ (calcd for $C_{37}H_{46}O_{12}Na$, 705.2887).

*Falcatin F (**6**):* amorphous solid; $[\alpha]^{25}_D$ +2 (*c* 0.1, $CHCl_3$); ^{1}H and ^{13}C NMR data, see Tables 1 and 2; HRESIMS *m*/*z* 691.3125 $[M + Na]^+$ (calcd for $C_{37}H_{48}O_{11}Na$, 691.3094), 686.3574 $[M + NH_4]^+$ (calcd for $C_{37}H_{52}NO_{11}$, 686.3540).

DOI: 10.1021/acs.jnatprod.6b00260
J. Nat. Prod. XXXX, XXX, XXX−XXX

Falcatin G (7): amorphous solid; $[\alpha]^{28}_{D}$ +20 (*c* 0.04, $CHCl_3$); ^1H and ^{13}C NMR data, see Tables 3 and 4; HRESIMS *m*/*z* 775.2986 $[M + H]^+$ (calcd for $C_{42}H_{47}O_{14}$, 775.2966).

Falcatin H (8): amorphous solid; $[\alpha]^{28}_{D}$ +57 (*c* 0.1, $CHCl_3$); ^1H and ^{13}C NMR data, see Tables 3 and 4; HRESIMS *m*/*z* 701.2815 $[M + Na]^+$ (calcd for $C_{34}H_{46}O_{14}Na$, 701.2785), 696.3270 $[M + NH_4]^+$ (calcd for $C_{34}H_{50}NO_{14}$, 696.3231).

Falcatin I (9): amorphous solid; $[\alpha]^{25}_{D}$ +63 (*c* 0.1, $CHCl_3$); ^1H and ^{13}C NMR data, see Tables 3 and 4; HRESIMS *m*/*z* 756.3264 $[M + H]^+$ (calcd for $C_{39}H_{50}NO_{14}$, 756.3231), 778.3083 $[M + Na]^+$ (calcd for $C_{39}H_{49}NO_{14}Na$, 778.3051).

Falcatin J (10): amorphous solid; $[\alpha]^{25}_{D}$ +108 (*c* 0.1, $CHCl_3$); ^1H and ^{13}C NMR data, see Tables 3 and 4; HRESIMS *m*/*z* 745.3078 $[M + Na]^+$ (calcd for $C_{36}H_{50}O_{15}$, 745.3047).

Falcatin K (11): amorphous solid; $[\alpha]^{25}_{D}$ +77 (*c* 0.1, $CHCl_3$); ^1H and ^{13}C NMR data, see Tables 3 and 4; HRESIMS *m*/*z* 759.3240 $[M + Na]^+$ (calcd for $C_{37}H_{52}O_{15}Na$, 759.3204).

Falcatin L (12): amorphous solid; $[\alpha]^{25}_{D}$ +30 (*c* 0.1, $CHCl_3$); ^1H and ^{13}C NMR data, see Tables 3 and 4; HRESIMS *m*/*z* 842.3640 $[M + H]^+$ (calcd for $C_{43}H_{56}NO_{16}$, 842.3599), 864.3463 $[M + Na]^+$ (calcd for $C_{43}H_{55}NO_{16}Na$, 864.3419).

Falcatin M (13): white powder; $[\alpha]^{28}_{D}$ +84 (*c* 0.2, $CHCl_3$); ^1H and ^{13}C NMR data, see Tables 5 and 6; HRESIMS *m*/*z* 828.3479 $[M + H]^+$ (calcd for $C_{42}H_{54}NO_{16}$, 828.3443), 850.3292 $[M + Na]^+$ (calcd for $C_{42}H_{53}NO_{16}Na$, 850.3262).

Falcatin N (14): amorphous solid; $[\alpha]^{25}_{D}$ +53 (*c* 0.1, $CHCl_3$); ^1H and ^{13}C NMR data, see Tables 5 and 6; HRESIMS *m*/*z* 814.3333 $[M + H]^+$ (calcd for $C_{41}H_{52}NO_{16}$, 814.3286), 836.3145 $[M + Na]^+$ (calcd for $C_{41}H_{51}NO_{16}Na$, 836.3106).

Falcatin O (15): amorphous solid; $[\alpha]^{25}_{D}$ +65 (*c* 0.1, $CHCl_3$); ^1H and ^{13}C NMR data, see Tables 5 and 6; HRESIMS *m*/*z* 827.3479 $[M + H]^+$ (calcd for $C_{43}H_{55}O_{16}$, 827.3490).

Falcatin P (16): amorphous solid; $[\alpha]^{28}_{D}$ −13 (*c* 0.04, $CHCl_3$); ^1H and ^{13}C NMR data, see Tables 5 and 6; HRESIMS *m*/*z* 741.3501 $[M + H]^+$ (calcd for $C_{40}H_{53}O_{13}$, 741.3486).

Falcatin Q (17): amorphous solid; $[\alpha]^{25}_{D}$ −16 (*c* 0.1, $CHCl_3$); ^1H and ^{13}C NMR data, see Table 5 and 6; HRESIMS *m*/*z* 790.3474 $[M + H]^+$ (calcd for $C_{43}H_{52}NO_{13}$, 790.3439), 812.3292 $[M + Na]^+$ (calcd for $C_{43}H_{51}NO_{13}Na$, 812.3258).

Falcatin R (18): amorphous solid; $[\alpha]^{25}_{D}$ −18 (*c* 0.2, $CHCl_3$); ^1H and ^{13}C NMR data, see Tables 6 and 7; HRESIMS *m*/*z* 776.3316 $[M + H]^+$ (calcd for $C_{42}H_{50}NO_{13}$, 776.3282), 798.3129 $[M + Na]^+$ (calcd for $C_{42}H_{49}NO_{13}Na$, 798.3102).

Falcatin S (19): amorphous solid; $[\alpha]^{25}_{D}$ −23 (*c* 0.1, $CHCl_3$); ^1H and ^{13}C NMR data, see Tables 6 and 7; HRESIMS *m*/*z* 748.3373 $[M + H]^+$ (calcd for $C_{41}H_{50}NO_{12}$, 748.3333), 770.3186 $[M + Na]^+$ (calcd for $C_{41}H_{49}NO_{12}Na$, 770.3152).

Euphorprolitherin D (20): amorphous solid; $[\alpha]^{25}_{D}$ +74 (*c* 0.1, $CHCl_3$); ^1H and ^{13}C NMR data identical with published data.[33]

Electrophysiological Investigations. GIRK and hERG ion currents were measured using planar patch-clamp technology with a four-channel medium throughput fully automated patch-clamp system (Patchliner, Nanion Technologies GmbH, Munich, Germany).[47] Whole-cell configuration was applied in all experiments. The pipetting protocols were controlled by PatchControlHT 1.07.50 software (Nanion Technologies GmbH). Current recordings and online analysis were performed with an EPC-10 Quadro patch-clamp amplifier (HEKA Elektronik Dr. Schulze GmbH) using the PatchMaster 2.43 software (HEKA Elektronik Dr. Schulze GmbH, Lambrecht/Pfalz, Germany).

Automated patch-clamp experiments were carried out at room temperature with a suspension of stable transfected cell lines. Suspensions of cells for measurements were derived from running cell cultures. Cells were maintained in an incubator at 37 °C, in 5% CO_2. Before experiments, cells were washed twice with PBS (Life Technologies Corporation, Carlsbad, CA, USA) and then detached with trypsin-EDTA (PAA Laboratories GmbH, Pasching, Austria) for 1−3 min. Trypsin was blocked with serum containing complete culture medium. The cell suspension was next centrifuged (2 min, 100*g*), resuspended in serum-free base medium at a final density of 1×10^6−5×10^6 cells/mL, and kept in the cell hotel of the Patchliner system. Cells were recovered after 15−30 min and remained suitable for automated patch-clamp recordings for up to 4 h.

Stocks of extra- and intracellular solutions were made for automated patch-clamp recordings. Chemicals were purchased from Sigma-Aldrich Corporation (St. Louis, MO, USA). All solutions were sterile filtered. Aliquots were stored at −20 °C and warmed to room temperature before use.

For each diterpene isolated from *E. falcata*, a stock solution of test compound (10 mM) was prepared. The solubilizing agent was dimethyl sulfoxide (DMSO, Sigma-Aldrich Corporation). Aliquots were stored at −20 °C. Before experiments, stock solutions were further diluted with high K^+ external solution (GIRK assay) or external solution (hERG assay) to give appropriate concentrations for the measurements. The final DMSO concentrations in the tested samples were 0.3% or less.

GIRK Channel Inhibitory Assay. Experiments were carried out on HEK-293 (human embryonic kidney) cells stably expressing GIRK1/4 (Kir3.1/3.4) K^+ channels.[48] This cell line originated from UCL Business PLC (London, UK). Cells were maintained in MEM (PAA Laboratories GmbH) medium supplemented with 10% FBS (fetal bovine serum) (PAA Laboratories GmbH) and 182 μg/mL zeocin (Life Technologies Corporation).

The following solutions were used during patch-clamp recordings (compositions in mM): external solution: NaCl 140, KCl 4, glucose-monohydrate 5, $MgCl_2$ 1, $CaCl_2$ 3, and HEPES 10 (pH 7.4, NaOH); high K^+ external solution: NaCl 135, KCl 25, $MgCl_2$ 1, $CaCl_2$ 3, and HEPES 10 (pH 7.4, NaOH); K^+-free external solution: NaCl 160, $MgCl_2$ 1, $CaCl_2$ 3, and HEPES 10 (pH 7.4, NaOH); internal solution: K-gluconate 40, NaCl 20, KF 60, EGTA 20, and HEPES 10 (pH 7.2, KOH), supplemented with 0.9 mM GTPγS (guanosine 5′-*O*-(γ-thio)triphosphate) before the experiments to induce channel activation.

The voltage protocol for the GIRK ion channel assay (see inset in panel C, Figure 6) started with a depolarizing voltage step to 60 mV for 100 ms before a 500 ms long hyperpolarizing ramp to −140 mV was applied. Then, the membrane potential remained at −140 mV for 100 ms before returning to the holding potential of −40 mV. The inward currents were calculated from the −140 mV segment. The pulse frequency was approximately 0.1 Hz.

At the beginning of the recordings, the normal external solution (4 mM K^+) was replaced with a high-K^+ external solution in order to increase the current amplitude. After 3 min of a control period, the test compounds were added to the cells in increasing concentrations (1 and 10 μM in the case of screening; 1, 3, 10, and 30 μM for each IC_{50} assay), for approximately 2 min. Propafenone (1 μM, Sigma-Aldrich Corporation) was used as a reference compound, and then potassium-free external solution was applied. The data were corrected with the current values measured in the potassium-free external solution, which served as the baseline.

hERG Channel Inhibitory Assay. hERG measurements were performed on HEK-293 cells stably transfected with cDNA encoding the hERG (Kv11.1) K^+ channel.[49] The cell line was purchased from Cell Culture Service (Hamburg, Germany). Cells were maintained in IMDM (Iscove's modified Dulbecco's medium) (PAA Laboratories GmbH) medium supplemented with 10% FBS (PAA Laboratories GmbH), 2 mM L-glutamine (Life Technologies Corporation), 1 mM Na-pyruvate (PAA Laboratories GmbH), and 500 μg/mL G418 (PAA Laboratories GmbH).

The following solutions were used during patch-clamp experiments (compositions in mM): external solution: NaCl 140, KCl 4, glucose-monohydrate 5, $MgCl_2$ 1, $CaCl_2$ 3, and HEPES 10 (pH 7.4, NaOH); internal solution: KCl 50, NaCl 10, KF 60, EGTA 20, and HEPES 10 (pH 7.2, KOH).

The voltage protocol for the hERG ion channel (see inset in panel A, Figure 6) started with a short (100 ms) −40 mV voltage step, as a reference. A 20 mV depolarizing step was applied for 3 s, and then the test potential was −40 mV for 1 s to evoke an outward tail current. The holding potential was −80 mV, and the pulse frequency was 0.1 Hz. The peak tail current was corrected with the leak current defined during the first period to −40 mV.

DOI: 10.1021/acs.jnatprod.6b00260
J. Nat. Prod. XXXX, XXX, XXX−XXX

The recording started in the external solution. After this control period, increasing concentrations of each test compound (3, 10, and 30 μM, respectively) were applied, each for approximately 3 min. Following test compound administration, 10 μM amitriptyline was applied as a reference inhibitor followed by a wash-out step.

■ ASSOCIATED CONTENT

Supporting Information

The Supporting Information is available free of charge on the ACS Publications website at DOI: 10.1021/acs.jnatprod.6b00260.

Representative 1D and 2D NMR spectra of the diterpenes isolated from *Euphorbia falcata* illustrating myrsinane-, cyclomyrsinane-, and premyrsinane-type polyesters (PDF)

■ AUTHOR INFORMATION

Corresponding Author

*Tel: +36-62-546453. Fax: +36-62-547404. E-mail: hohmann@pharm.u-szeged.hu.

Notes

The authors declare no competing financial interest.

■ ACKNOWLEDGMENTS

Financial support from the Hungarian Scientific Research Fund (OTKA K109846) is gratefully acknowledged. A.V. acknowledges the award of a János Bolyai scholarship of the Hungarian Academy of Sciences.

■ REFERENCES

(1) http://apps.who.int/iris/bitstream/10665/200009/1/9789241565110_eng.pdf.
(2) Dunlop, J.; Bowlby, M.; Peri, R.; Vasilyev, D.; Arias, R. *Nat. Rev. Drug Discovery* **2008**, *7*, 358−368.
(3) Farre, C.; Stoelzle, S.; Haarmann, C.; George, M.; Brüggemann, A.; Fertig, N. *Expert Opin. Ther. Targets* **2007**, *11*, 557−565.
(4) Farre, C.; Fertig, N. *Expert Opin. Drug Discovery* **2012**, *7*, 515−524.
(5) Farre, C.; Haythornthwaite, A.; Haarmann, C.; Stoelzle, S.; Kreir, M.; George, M.; Brüggemann, A.; Fertig, N. *Comb. Chem. High Throughput Screening* **2009**, *12*, 24−37.
(6) Lü, Q.; An, W. F. *Comb. Chem. High Throughput Screening* **2008**, *11*, 185−194.
(7) Stoelzle, S.; Obergrussberger, A.; Brüggemann, A.; Haarmann, C.; George, M.; Kettenhofen, R.; Fertig, N. *Front. Pharmacol.* **2011**, *2*, Article 76, 1−11.
(8) Zheng, W.; Spencer, R. H.; Kiss, L. *Assay Drug Dev. Technol.* **2004**, *2*, 543−552.
(9) Priest, B. T.; Swensen, A. M.; McManus, O. B. *Curr. Pharm. Des.* **2007**, *13*, 2325−2337.
(10) Willumsen, N. J.; Bech, M.; Olesen, S.-P.; Jensen, B. S.; Korsgaard, M. P. G.; Christophersen, P. *Recept. Channels* **2003**, *9*, 3−12.
(11) Dabrowski, M. A.; Dekermendjian, K.; Lund, P.-E.; Krupp, J. J.; Sinclair, J.; Larsson, O. *CNS Neurol. Disord.: Drug Targets* **2008**, *7*, 122−128.
(12) Treherne, J. M. *Curr. Pharm. Des.* **2006**, *12*, 397−406.
(13) Walsh, K. B. *Front. Pharmacol.* **2011**, *2*, Article 64, 1−8.10.3389/fphar.2011.00064
(14) Dobrev, D.; Friedrich, A.; Voigt, N.; Jost, N.; Wettwer, E.; Christ, T.; Knaut, M.; Ravens, U. *Circulation* **2005**, *112*, 3697−3706.
(15) Hashimoto, N.; Yamashita, T.; Tsuruzoe, N. *Pharmacol. Res.* **2006**, *54*, 136−141.
(16) Kobayashi, T.; Ikeda, K. *Curr. Pharm. Des.* **2006**, *12*, 4513−4523.
(17) Sanguinetti, M. C.; Tristani-Firouzi, M. *Nature* **2006**, *440*, 463−469.
(18) Farre, C.; George, M.; Brüggemann, A.; Fertig, N. *Drug Discovery Today: Technol.* **2008**, *5*, e23−e28.
(19) Abi-Gerges, N.; Holkham, H.; Jones, E. M. C.; Pollard, C. E.; Valentin, J.-P.; Robertson, G. A. *Br. J. Pharmacol.* **2011**, *164*, 419−432.
(20) Polonchuk, L. *Front. Pharmacol.* **2012**, *3*, Article 3, 1−7.10.3389/fphar.2012.00003
(21) Vasanthi, H. R.; ShriShriMal, N.; Das, D. K. *Curr. Med. Chem.* **2012**, *19*, 2242−2251.
(22) Vasas, A.; Hohmann, J. *Chem. Rev.* **2014**, *114*, 8579−8612.
(23) Xu, Z. H.; Sun, J.; Xu, R. S.; Qui, G. W. *Phytochemistry* **1998**, *49*, 149−151.
(24) Corea, G.; Fattorusso, E.; Lanzotti, V.; Taglialatela-Scafati, O.; Appendino, G.; Ballero, M.; Simon, P. N.; Dumontet, C.; Di Pietro, A. *J. Med. Chem.* **2003**, *46*, 3395−3402.
(25) Vasas, A.; Sulyok, E.; Martins, A.; Rédei, D.; Forgo, P.; Kele, Z.; Zupkó, I.; Molnár, J.; Pinke, G.; Hohmann, J. *Tetrahedron* **2012**, *68*, 1280−1285.
(26) Sulyok, E.; Vasas, A.; Rédei, D.; Forgo, P.; Kele, Z.; Pinke, G.; Hohmann, J. *Tetrahedron* **2011**, *67*, 7289−7293.
(27) Xu, J.; Yang, B.; Fang, L.; Wang, S.; Guo, Y.; Yamakuni, T.; Ohizumi, Y. *J. Nat. Med.* **2013**, *67*, 333−338.
(28) Li, J.; Xu, L.; Wang, F. P. *Helv. Chim. Acta* **2010**, *93*, 746−752.
(29) Xu, J.; Guo, Y.; Xie, C.; Li, Y.; Gao, J.; Zhang, T.; Hou, W.; Fang, L.; Gui, L. *J. Nat. Prod.* **2011**, *74*, 2224−2230.
(30) Ahmad, V. U.; Hussain, H.; Jassbi, A. R.; Hussain, J.; Bukhari, I. A.; Yasin, A.; Aziz, N.; Choudhary, M. I. *J. Nat. Prod.* **2003**, *66*, 1221−1224.
(31) Abbas, M.; Jassbi, A. R.; Zahid, M.; Ali, Z.; Alam, N.; Akhtar, F.; Choudhary, M. I.; Ahmad, V. U. *Helv. Chim. Acta* **2000**, *83*, 2751−2755.
(32) Ahmad, V. U.; Hussain, J.; Hussain, H.; Jassbi, A. R.; Ullah, F.; Lodhi, M. A.; Yasin, A.; Choudhary, M. I. *Chem. Pharm. Bull.* **2003**, *51*, 719−723.
(33) Zhang, W. J.; Chen, D. F.; Hou, A. J. *Chin. J. Chem.* **2004**, *22*, 103−108.
(34) Jeske, F.; Jakupovic, J.; Berendsohn, W. *Phytochemistry* **1995**, *40*, 1743−1750.
(35) Shi, Q. W.; Su, X. H.; Kiyota, H. *Chem. Rev.* **2008**, *108*, 4295−327.
(36) Ghanadian, S. M.; Ayatollahi, A. M.; Mesaik, M. A.; Abdalla, O. M. *Nat. Prod. Res.* **2013**, *27*, 246−254.
(37) Ghanadian, M.; Choudhary, M. I.; Ayatollahi, A. M.; Mesaik, M. A.; Abdalla, O. M.; Afsharypour, S. *J. Asian Nat. Prod. Res.* **2013**, *15*, 22−29.
(38) Ghanadian, S. M.; Ayatollahi, A. M.; Afsharypuor, S.; Javanmard, S. H.; Dana, N. *J. Nat. Med.* **2013**, *67*, 327−332.
(39) Shokoohinia, Y.; Sajjadi, S. E.; Zolfaghari, B.; Chianese, G.; Appendino, G.; Taglialatela-Scafati, O. *Fitoterapia* **2010**, *81*, 884−890.
(40) Xu, J.; Jin, D.; Song, H.; Guo, Y.; He, Y. *Fitoterapia* **2012**, *83*, 1205−1209.
(41) Wu, D. G.; Sorg, B.; Hecker, E. *Phytother. Res.* **1994**, *8*, 95−99.
(42) Ayatollahi, A. M.; Ghanadian, M.; Mesaik, A.; Abdella, O. M.; Afsharypuor, S.; Kobarfard, F.; Mirza-Taheri, M. *J. Asian Nat. Prod. Res.* **2010**, *12*, 1020−1025.
(43) Yu, J.; Jin, D.; Guo, P.; Xie, C.; Fang, L.; Guo, Y. *Molecules* **2012**, *17*, 9520−9528.
(44) Xu, J.; Guo, Y.; Xie, C.; Li, Y.; Gao, J.; Zhang, T.; Hou, W.; Fang, L.; Gui, L. *J. Nat. Prod.* **2011**, *74*, 2224−2230.
(45) Xu, J.; Jin, D.; Guo, Y.; Xie, C.; Ma, Y.; Yamakuni, T.; Ohizumi, Y. *Bioorg. Med. Chem. Lett.* **2012**, *22*, 3612−3618.
(46) Li, J.; Xu, L.; Wang, F. P. *Helv. Chim. Acta* **2010**, *93*, 746−752.
(47) http://nanion.de/images/stories/pdf/patchliner.pdf.
(48) Lajter, I.; Vasas, A.; Orvos, P.; Bánsághi, S.; Tálosi, L.; Jakab, G.; Béni, Z.; Háda, V.; Forgo, P.; Hohmann, J. *Planta Med.* **2013**, *79*, 1736−1741.
(49) Orvos, P.; Virág, L.; Tálosi, L.; Hajdú, Z.; Csupor, D.; Jedlinszki, N.; Szél, T.; Varró, A.; Hohmann, J. *Fitoterapia* **2015**, *100*, 156−165.

DOI: 10.1021/acs.jnatprod.6b00260
J. Nat. Prod. XXXX, XXX, XXX−XXX